SKI Report 2006:36

Research

Mechanical Integrity of Canisters Using a Fracture Mechanics Approach

Tomofumi Koyama
Guoxiang Zhang
Lanru Jing

July 2006

ISSN 1104-1374
ISRN SKI-R-06/36-SE

SKI perspective

Background

In the current plans for the disposal of spent nuclear fuel in Sweden a copper canister is intended to be used. The mechanical integrity is given by an iron insert, while the outer copper shell gives corrosion protection.

The canister must be shown to withstand high pressure (during glaciations) as well as shear displacements in the rock. Earlier SKB and SKI work on canister integrity has been using FEM analysis of elastoplastic deformation. To get a better understanding of the influence of fracture initiation and growth in the insert, a fracture mechanics approach will be used.

The Boundary Element Method (BEM) is an numerical approach efficient for modelling fracture initiation and fracture growth. It can also be used for modelling contact and thermo-elastic stresses. For modelling of coupled temperature-stress-flow in the bentonite and fractured rock surrounding the canister, a FEM approach is more suitable. Thus a combined BEM/FEM approach will be used to study the coupled system of canister/bentonite/rock.

Purpose of the project

The purpose with the current project is to:

- develop numerical modelling capabilities for SKI to study the potential threats to mechanical integrity of the canisters using fracture mechanics approach as a complement to continuous deformation methods used before
- prepare SKI in needs for knowledge and understanding of key technical issues reviewing SKB's studies on mechanical integrity of canisters.

The objectives of the project are:

- to investigate the possibility of initiation and growth of fractures in the cast-iron canisters under the mechanical loading conditions defined in the premises of canister design by Swedish Nuclear Fuel and Waste Management Co.
- to investigate the maximum bearing capacity of the cast-iron canisters under uniformly distributed and gradually increasing boundary pressure until plastic failure.

Results

The results of the BEM simulations, using the commercial code BEASY, indicate that under the currently defined loading conditions the possibility of initiation of new fractures or growth of existing fractures (defects) are very small, due to the reasons that the canisters are under mainly compressive stresses and the induced tensile stress regions are too small in both dimension and magnitude to create new fractures or to induce growth of existing fractures, besides the fact that the toughness of the fractures in the cast iron canisters are much higher that the stress intensity factors in the fracture tips.

The results of the FEM simulation show a approximately 75 MPa maximum pressure beyond which plastic collapse of the cast-iron canisters may occur, using an elasto-plastic material model. This figure is smaller compared with other figures obtained by SKB due to the reason that the FEM code (ADINA) has a different convergence iteration tolerance which prevents further increase of the load, and is therefore subjective to the numerical techniques applied for the plastic deformation analysis. A different maximum pressure may be possible if different convergence tolerance is adopted.

Effects on SKI work

This work will be used in the SKI evaluation of the SKB work on canister integrity. The report will also be used as one basis in SKI's forthcoming reviews of SKB's safety assessments of long-term safety and RD&D programmes.

Project information

Responsible for the project at SKI has been Christina Lilja.
SKI reference: SKI 2004/198/200509003

SKI Report 2006:36

Research

Mechanical Integrity of Canisters Using a Fracture Mechanics Approach

Tomofumi Koyama
Guoxiang Zhang
Lanru Jing

Group of Engineering Geology
Department of Land and Water Resources Engineering
Royal Institute of Technology
SE-100 44 Stockholm

July 2006

Summary

This report presents the methods and results of a research project for Swedish Nuclear Power Inspectorate (SKI) about numerical modeling of mechanical integrity of cast-iron canisters for the final disposal of spent nuclear fuel in Sweden, using combined boundary element (BEM) and finite element (FEM) methods.

The objectives of the project are: 1) to investigate the possibility of initiation and growth of fractures in the cast-iron canisters under the mechanical loading conditions defined in the premises of canister design by Swedish Nuclear Fuel and Waste Management Co. (SKB); 2) to investigate the maximum bearing capacity of the cast-iron canisters under uniformly distributed and gradually increasing boundary pressure until plastic failure. Achievement of the two objectives may provide some quantitative evidence for the mechanical integrity and overall safety of the cast-iron canisters that are needed for the final safety assessment of the geological repository of the radioactive waste repository in Sweden.

The geometrical dimension, distribution and magnitudes of loads and material properties of the canisters and possible fractures were provided by the latest investigations of SKB.

The results of the BEM simulations, using the commercial code BEASY, indicate that under the currently defined loading conditions the possibility of initiation of new fractures or growth of existing fractures (defects) are very small, due to the reasons that: 1) the canisters are under mainly compressive stresses; 2) the induced tensile stress regions are too small in both dimension and magnitude to create new fractures or to induce growth of existing fractures, besides the fact that the toughness of the fractures in the cast iron canisters are much higher that the stress intensity factors in the fracture tips.

The results of the FEM simulation show a approximately 75 MPa maximum pressure beyond which plastic collapse of the cast-iron canisters may occur, using an elasto-plastic material model. This figure is smaller compared with other figures obtained by SKB due to the reason that the FEM code (ADINA) has a different convergence iteration tolerance which prevents further increase of the load, and is therefore subjective to the numerical techniques applied for the plastic deformation analysis. A different maximum pressure may be possible if different convergence tolerance is adopted.

Content

1. INTRODUCTION

For the mechanical integrity of canisters for nuclear waste disposal, the numerical modelling works so far have focused on continuous deformation of the canisters as either a whole or its parts (such as lid and cylinder). Initiation and potential growth of fractures has not been investigated by using either numerical modelling or experiments. The issue of fracturing may become significant especially when the defects are located at some critical places of the cast iron insert. It has been noted in the past that mechanical safety of canisters depends on not only its deformation or stress, but the potential of fracture initiation and growth under possible extreme loading conditions, since formation of fractures or growth of defects will lead to the loss of functionality of the canister no matter its deformation is small or large. A canister keeping its mechanical integrity without holes or fractures may still serve as an isolation barrier to a certain extent, even if its deformation is large. Research on potential fracturing process of the canister as a whole or any integral parts of it is also needed. The most obvious way ahead is then the fracture mechanics approach instead of continuous deformation approach.

An efficient numerical approach dealing with fracture initiation and growth issues is the Boundary Element Method (BEM) since its efficiency for direct accommodation of fracture initiation and growth without artificial re-meshing difficulties as encountered when a FEM approach is used. The non-linear behaviour of the canister and fractured rocks, such as plastic deformation and fracturing, is most efficiently modelled using FEM based on continuum approach.

The above concepts are the basis for the current project for numerical modelling of mechanical integrity of canisters. The aims of the project are:

i) Testing the proposed test cases in the SKB's canister design premises with the alternative bentonite swelling pressure distributions to examine the risks of the fracturing processes, by placing one or a few number of hypothetic defects in sensitive locations in the canister and observe its possible development and potential effect on the mechanical integrity of the canister, using a linear elastic fracture mechanics approach with the BEM code (BEASY). The problem was considered as three-dimensional, but with symmetry conditions considered whenever the geometry and boundary conditions permit.

ii) Testing the collapse load of the cast iron insert, using an elasto-plastic approach with a FEM code ADINA. The problem was considered as two-dimensional with a 1/8 symmetry for both geometry and loading condition.

The canister design geometry and loading cases as defined in Werme (1998). Only the BWR types of cast iron insert was considered since it represents the more risky cases.

2. THE LOADING CASES

The main loading conditions considered are the two cases in the canister design premises defined in Werme (1998), with differential mobilization of swelling pressure (see Fig. 1), one case with possible deviations of fuel hole positions (thus causing unsymmetric geometry and change of thickness of the separation of the cast iron insert, another case of a generic simulation for defining the utmost collapsing loads required to produce plastic deformation using FEM. In theory, the loading cases should apply to both PWR and BWR types of canisters, buit only the BWR type was considered since this geometry is the more risky type with more fuel holes.

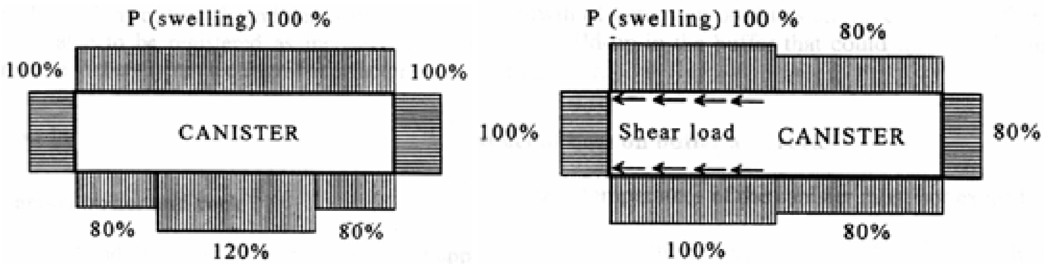

(a) (b)

Figure 1. Two extreme loading cases of uneven distribution of swelling pressure considered for canister design (Werme, 1998).

A different loading case considered in SKB design and analysis of canister safety is a 200 mm shear displacement along a fracture in rock, intersecting the canister. For this case, the locations of the rock fracture and its orientation, and the bentonite deformation with dry, partial or full saturation should be incorporated. Due to such complexity this loading case is not considered in this report.

For all the cases, the modeling starts with stress analysis without fractures. Results will indicate the critical locations with largest tensile stress concentrations. An initial fracture can then be inserted to the locations with tensile stresses under the same loading conditions to examine its potential for growth.

Loading case (a) (Fig. 1a)

The swelling pressure is fully developed (with 44 MPa) on one side of the canister's cylindrical surface and on the end surfaces. On the other side of the cylindrical surface, the swelling pressure is 20% of the mobilized along the central half and 20% reduced along the remaining quarters at the ends of the canister. Due to the non-symmetric loading conditions, a 3D model with a 1/4 canister is required.

Loading case (b) (Fig. 1b)

The swelling pressure is fully developed around the bottom half of the canister, while the swelling pressure is 20% lower around the top half. The resulting upward force, which results from the differences in pressure against the canister's end surface, is balanced by a shear force along the bottom half of the cylindrical surface.

c) Loading case (c) (Fig. 2)

This loading case was considered for possible effects of deviation of the fuel hole positions from the design. A shift of 1, 2, 5 and 10 mm of the fuel hole location in one direction is considered (Fig. 2) so that the original thickness of separation d is changed. The load on the outer surface is 44 MPa of the maximum design load.

d) Loading case (d)

This case is defined for a generic study of the utmost collapsing loads the cast iron insert may bear without any initial defective fracture. A uniformly distributed external load will be increased incrementally until the insert loses its structural stability with plastic flow. Full symmetric condition should be used for the BWR type, without considering the inner tubes inside the fuel holes and the copper shell. The radius of the corner of the fuel holes should be considered with the latest design considerations.

The above loading cases are considered to represent minimum requirements considering only one case of fracture number, size and location, and one case of the radius of the corners of the fuel holes in the cast iron insert.

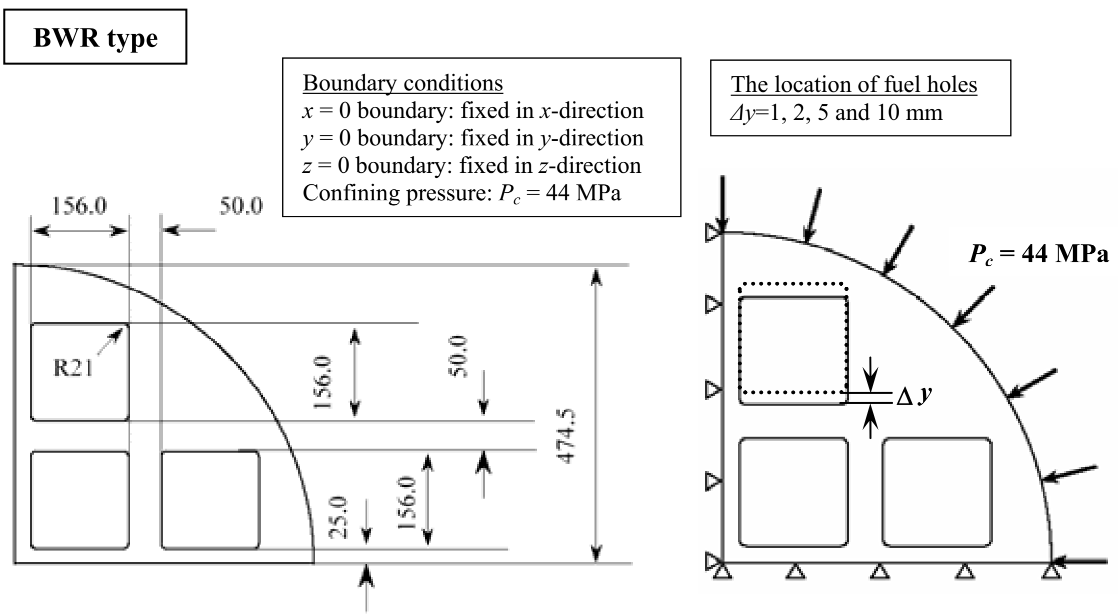

a) Boundary conditions for sensitivity analysis for BWR type

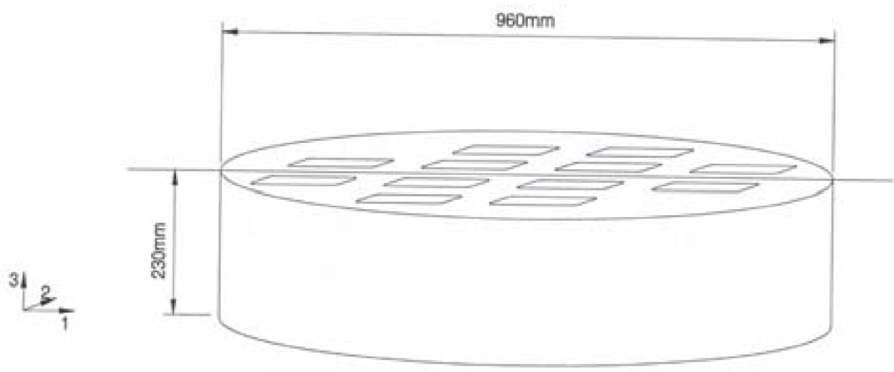

b) A slice of 230 mm in thickness for the 3D model geometry

Figure 2. Model geometry and loading condition for loading case (c) -BWR type.

3. MATERIAL PROPERTIES

The elastic properties of the cast iron are the Young's modulus (E) and Poisson's ratio (ν), given by E = 170 GPa and $\nu = 0.3$. The fracture toughness parameters are listed in Table 1, which is obtained form measured data at the Solid Mechanics Division at KTH (Nilsson, 2005).

Table 1 Fracture toughness parameters for Mode I fracture.

Parameters	J_{IC} value	Parameters	K_{IC} value
J_{IC} (+23 ºC, mean) [kN/m]	47.1	K_{IC} (+23 ºC, mean) [MN/mm$^{3/2}$]	2.964
J_{IC} (0 ºC, mean) [kN/m]	28.5	K_{IC} (0 ºC, mean) [MN/mm$^{3/2}$]	2.306
Initial fracture length [mm]	1, 2, 5 and 10		

The K_{IC} values are calculated from J_{IC} values using the following equation (Broek, 1986)

$$J_{IC} = \frac{1-\nu^2}{E} K_{IC} \tag{1}$$

The plastic material properties are described in Chapter 5 for loading case d), where it is more appropriate.

To help readers unfamiliar with concepts of fracture mechanics in use of the above parameters for fracture growth modeling, a short description is given below.

In the linear elastic fracture mechanics, the fundamental postulate is that the fracture behaviour is determined by only the values of the stress intensity factors (SIF) which are a function of the applied load and the geometry of the fractured structure (Broek, 1986). The stress intensity factors thus play a fundamental role in linear elastic fracture mechanics applications.

Fracture growth processes are simulated through an incremental fracture extension process. For each increment of the fracture extension, a stress analysis is carried out and the stress intensity factors are evaluated. The crack path is computed by a criterion defined in terms of the stress intensity factors.

In general, numerical methods were used for the evaluation of the stress intensity factors around the crack tip. In the BEASY code, the stress intensity factors are computed using opening displacement method for the 3D problems. The calculated stress intensity factors around the crack tips are compared with the critical values of the fracture toughness. Fracture extension will take place if the calculated stress inensity factors, K exceeds a critical value, K_C. It should be noted that in most of fracturing processes, the role of shear modes (mode II and III) will be subordinate to that of the tensile mode (mode I). Hence, the calculated stress intensity factor for the mode I, K_I is always compared with a critical value, K_{IC}.

In determination of fracture toughness in lab, instead of evaluating directly the K values, the values of the so called J integral is often used as a fracture criterion, The critical value J_{IC} is measured during the toughness tests, and J is interpreted as an energy release rate. The fracture will propagate if values of J exceed J_{IC}. The K_{IC} and J_{IC} values are related through equation (1) and this relation is valid for the linear elastic fracture mechanics applications.

4. RESULTS OF FRACTURING POTENTIALS

The presentation of the numerical simulation is given in the order of loading cases c)-a)-b)-d) with increasing complexity in either model geometry, loading condition or material behaviour.

4.1 Results of loading case c)

Figure 3 shows the BEM mesh for the model with loading case c), for pure stress calculations without fractures. The boundary condition is a 44 MPa radial load on the outer surface as shown in Fig. 2a. A 1/4 geometric symmetry was assumed.

Figures 4-10 present the 3D distributions of the maximum principle stress (σ_1), Von Mises effective stress, and displacement as iso-value contour maps, for the cases of no-deviation of the fule hole position, and with 1mm, 2mm, 5mm and 10mm shifting in the *y*-direction, respectively. It is shown that with no such deviations, the maximum tensile stress of small magnitude (< 65 MPa) occurs on the wall of the the two fule holes closest to the outer surface of the insert and the maximum Von Mises effective stress of also small magnitude (< 460 MPa) occurs at the two corners of the same two fuel holes, respectively. With such small magnitudes of tensile stress and Von Mises effective stress, it is not likely that any fracture could initiate at all, and no existing fractures with given toughness in Table 1 will grow either. However, for confidence in results and evaluation, four fractures were inserted on the wall and at the corners of the two fule holes (Fig.11) where maximum tensile stresses are found, and simulation of the possible growth of these fractures were conducted. Figure 11 a and b indicate their general locations in the BEM mesh and Figure 11c shows the details of the fracture geometry and mesh before loading is started. The initial length of the fractures (defects) are assumed to be 1, 2, 5 and 10 mm, respectively to test the sensitivities of fracture growth with fracture size (Fig.12).

The results of the analysis, as the SIF (stress intensity factor) for three modes of fracturing at the mesh points (MP) along the tips of inserted initial fractures as manufacturing defects, are presented in Tables A1-A20 in the Appendex as calculated stress intensity factor (SIF) at the crack tip mesh points with initial crack size of 1, 2, 5 and 10mm, for the case without fuel hole deviation, and with deviations of 1, 2, 5 and 10mm, in the *y*-direction, respectively. Observation of these tables indicate that all SIF at these fracture tips are less than the K_{IC} value in Table 1. The fractures in all cases therefore do not grow, due to mainly two reasons: 1) fracture toughness of the cast iron is adequately high; 2) the magnitude and distribution areas of the tensile stresses are very small. Therefore there is no enough mobilized energy by the tensile stress field to overcome the resistence of the fracture toughness in order to create additional fracture surfaces from the tip front to make the area of existent fracture increase (fracture grow).

Note that the numbers of mesh point in Tables A1-A20 are not the real node numbers in the BEASY models for this set of calculation. These node numbers changes with changing fracture size and location in each model, but the total number of mesh point along each fracture are the same (15 points). Therefore the same geometrical locations and numbering of these points as shown in Fig. 13 are used to indicate their locations and order, for all cases of loading case c) in order to avoid repetitive drawing of the same plots.

When initial fractures are inserted into the models, their tips may sometimes penetrate into compression stress areas if their initial size is larger than the thickness of the tensile stress zone (which is usually very thin as shown in Figs. 4 and 6). This penetration is one of the reasons that negative SIF values were obtained at many mesh points along fracture tips due to the dominance of nearby compressive stress fields, due to the special sign convention used in the BEASY code when the SIF is calculated.

In comparison between the simulated cases, the case of fracture of 1 mm in size with or without fuel hole position deviation generates maximum value of SIF, indicating this case is the closest condition toward possible fracturing, but still far from reaching a critical state for fracture growth.

In general, this set of simulation results show that no crack growth will be caused due to deviation of fuel hole deviations up to 10 mm, in either *y*- or *z*-direction (due to symmetric geometry of the canister), due to dominance of the compressive stress field, small magnitude of tensile stresses on the wall of fuel holes, and adequate fracture toughness of the cast iron. This conclusion may be extended to general deviations of fuel holes no more than 10 mm due to the same reasons as mentioned above, since such deviations will not likely generate very extensive distributions of tensile stresses of very large magnitude.

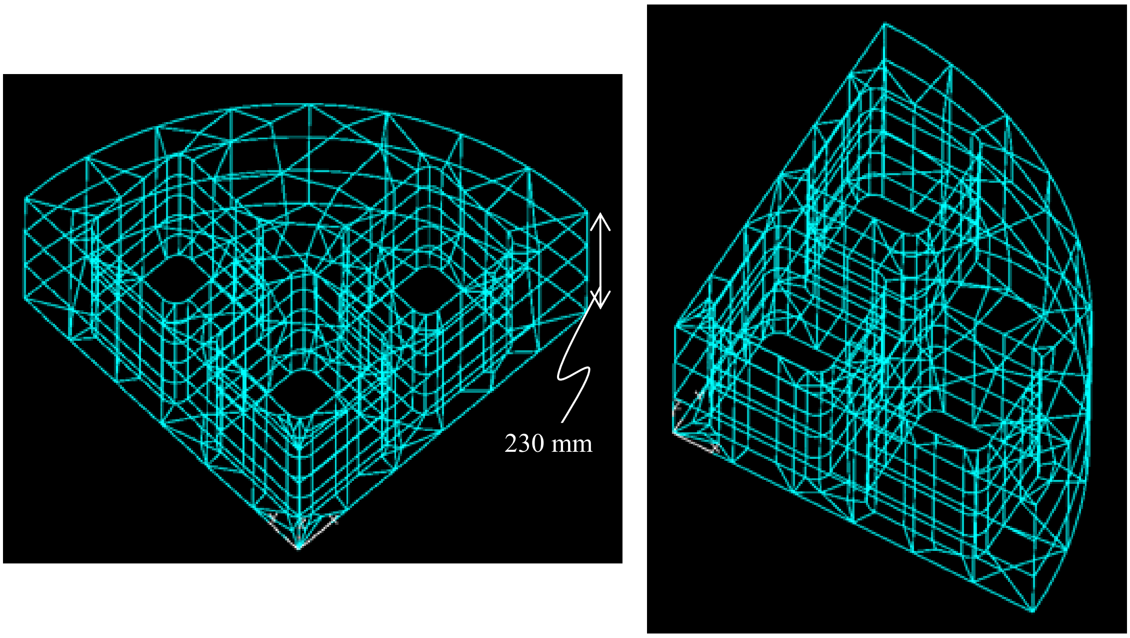

Figure 3. Calculation mesh of a slice of BWR type canister using BEASY code (for stress calculation).

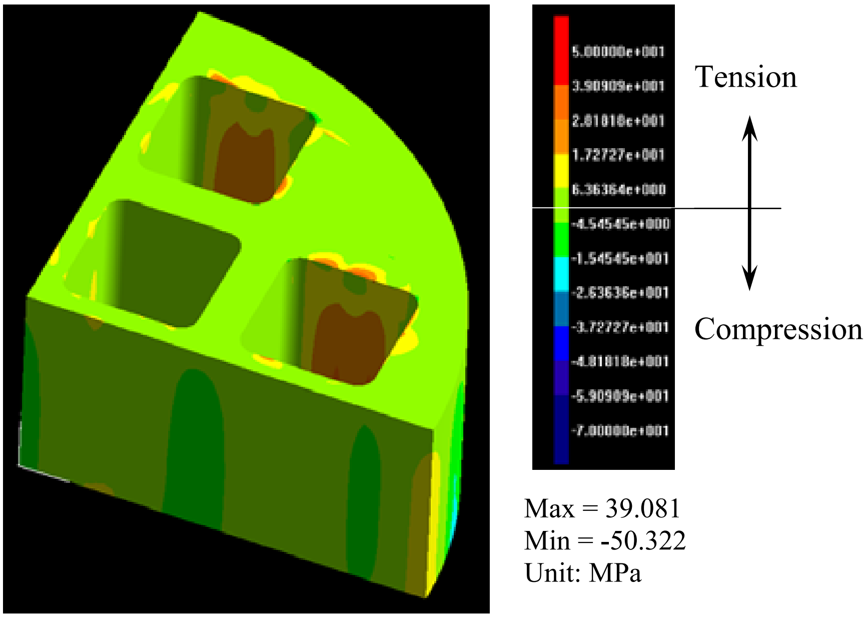

a)

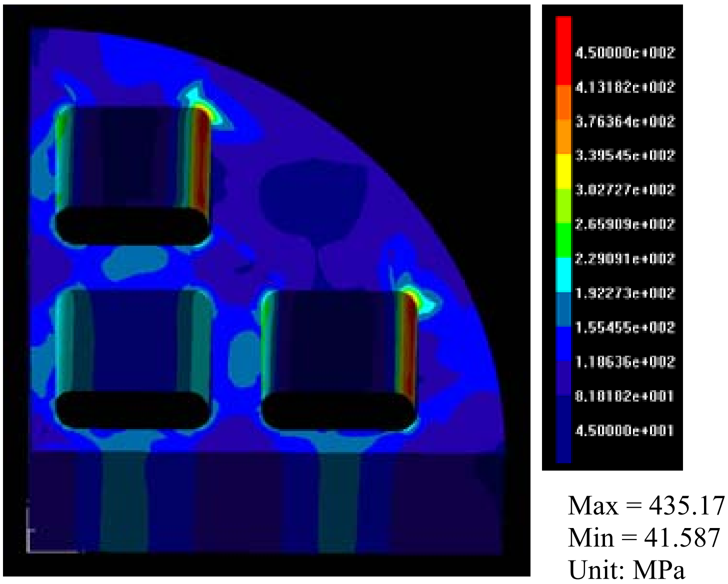

b)

Figure 4. Results of stress analysis for BWR type canister without movement of the fuel hole location, a) maximum principle stress (σ_1 plot) and b) von Mises effective stress.

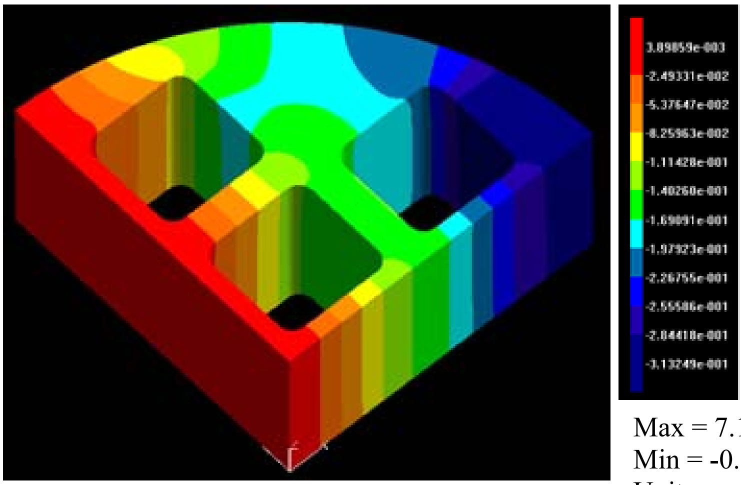

Max = 7.13479E-3
Min = -0.31649
Unit: mm

a)

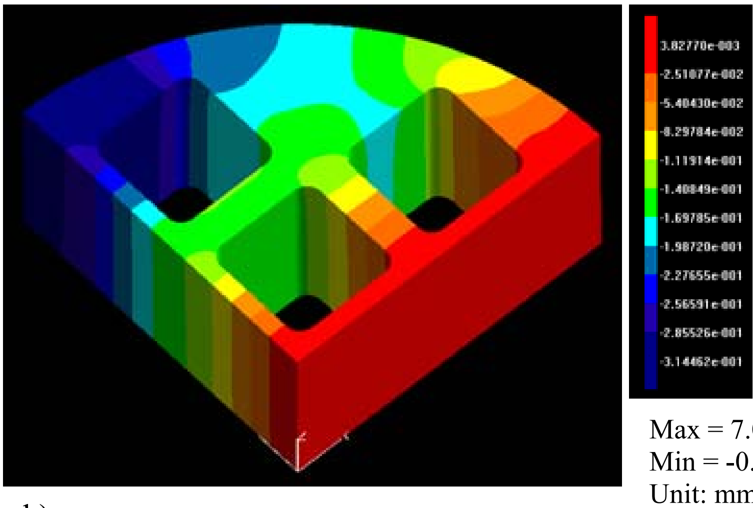

Max = 7.07555E-3
Min = -0.31771
Unit: mm

b)

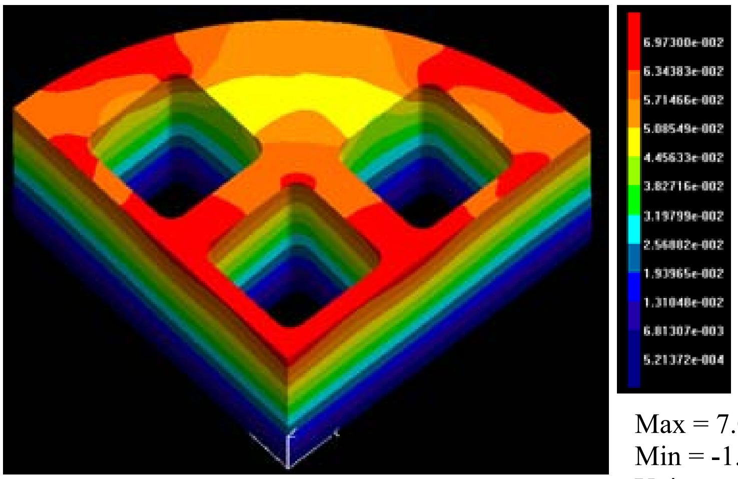

Max = 7.04362E-3
Min = -1.84839E-4
Unit: mm

c)

Figure 5. Displacement of BWR type canister without movement of the fuel hole location in the a) *x*-, b) *y*-and b) *z*-directions.

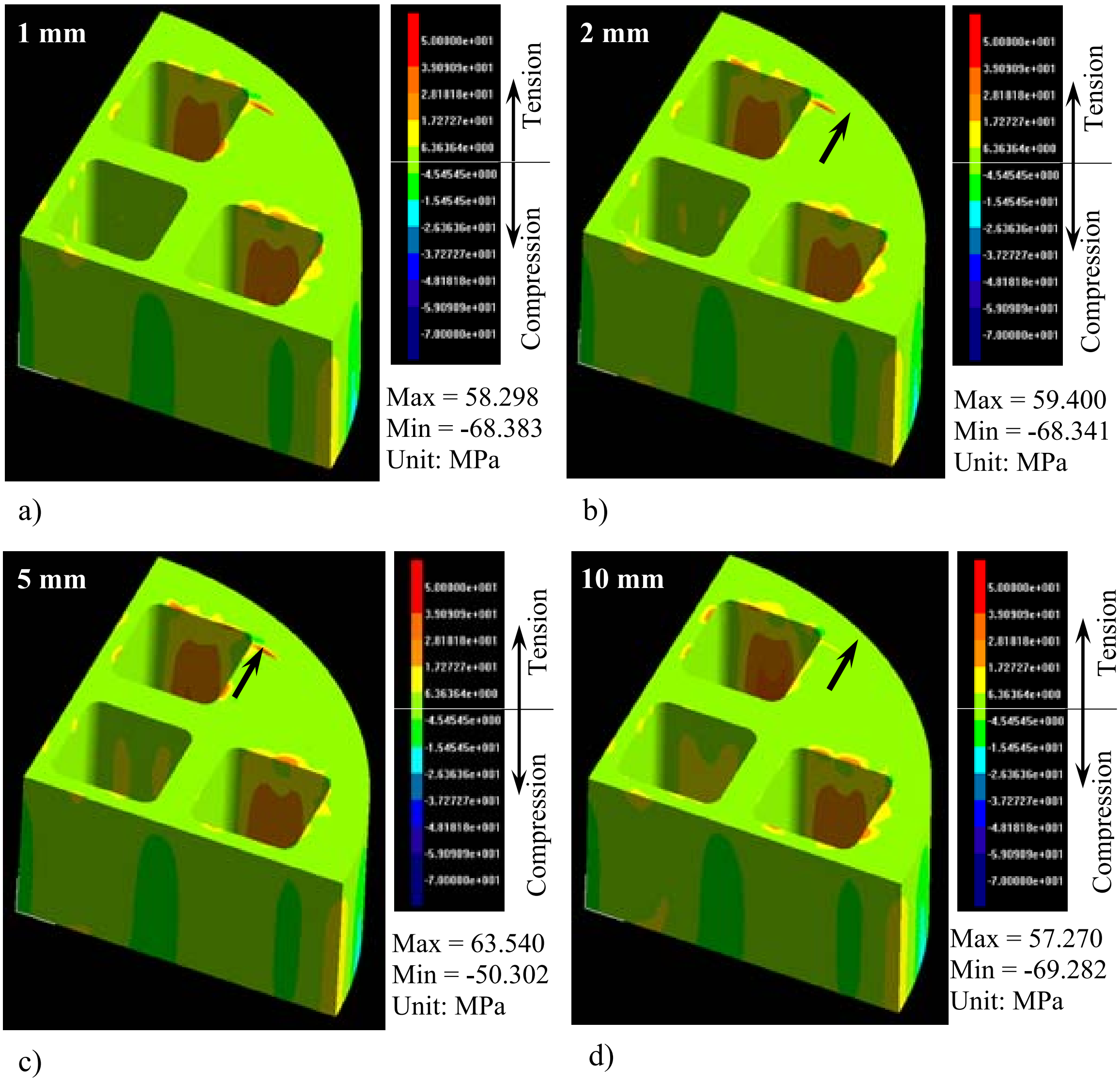

Figure 6. Results of stress analysis (maximum principle stress, σ_1 plot) for sensitivity analysis in terms of the fuel location, a) 1 mm, b) 2 mm, c) 5 mm and d) 10 mm dislocations.

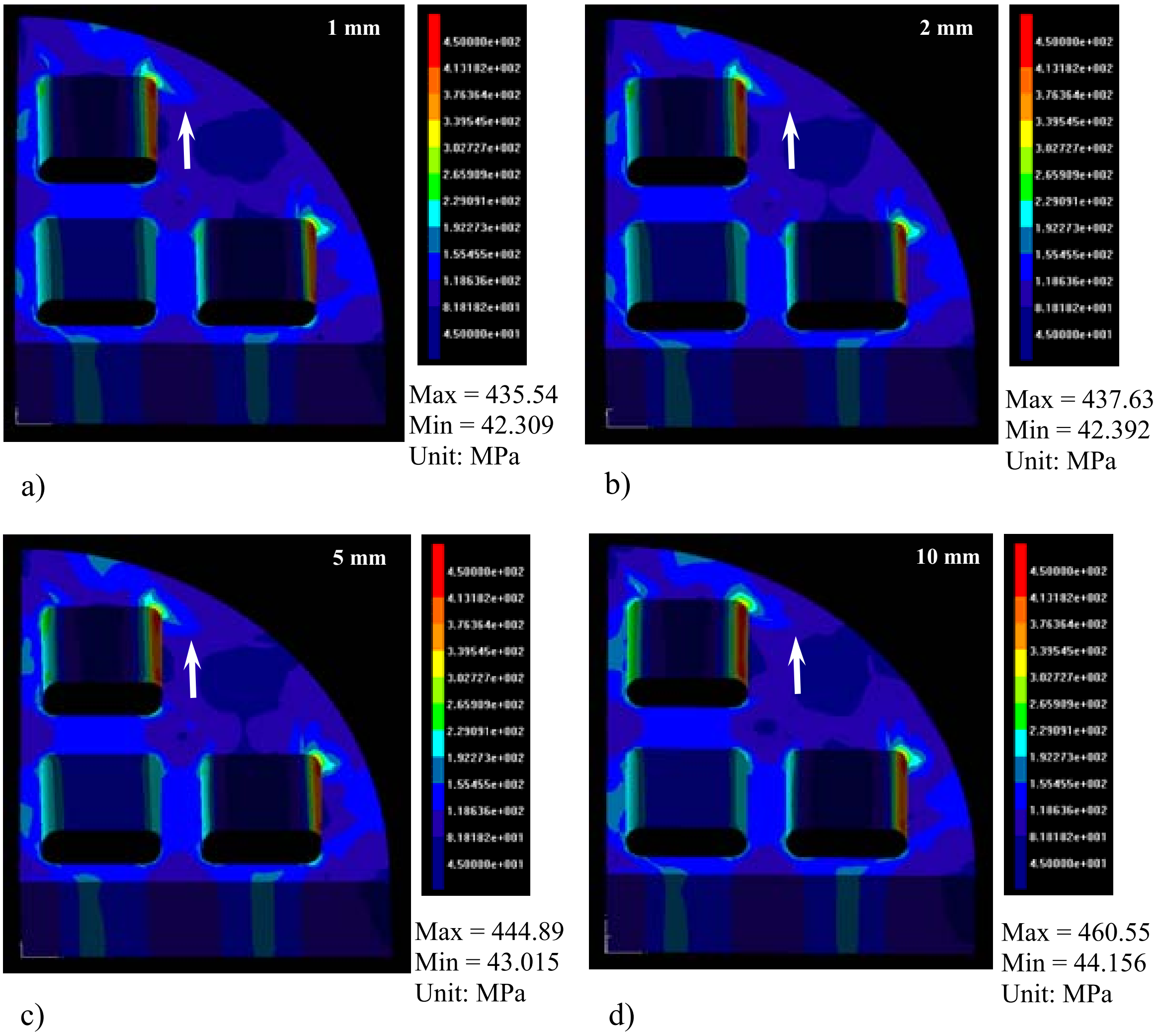

Figure 7. Results of stress analysis (von Mises effective stress) for sensitivity analysis in terms of the fuel location, a) 1 mm, b) 2 mm, c) 5 mm and d) 10 mm movements.

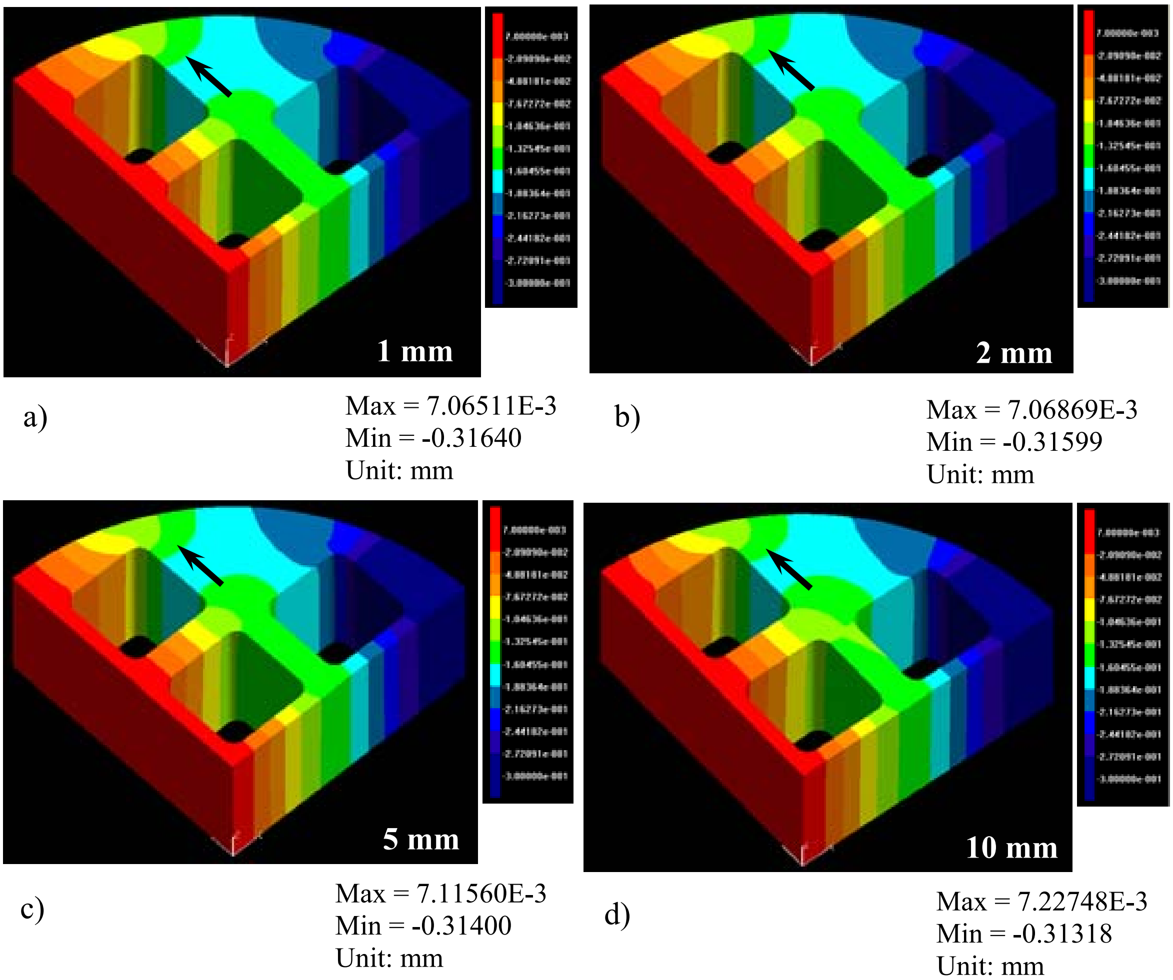

Figure 8. Displacement of BWR type canister in the *x*-direction with deviation of the fuel hole location by a) 1 mm, b) 2 mm, c) 5 mm and d) 10 mm, respectively.

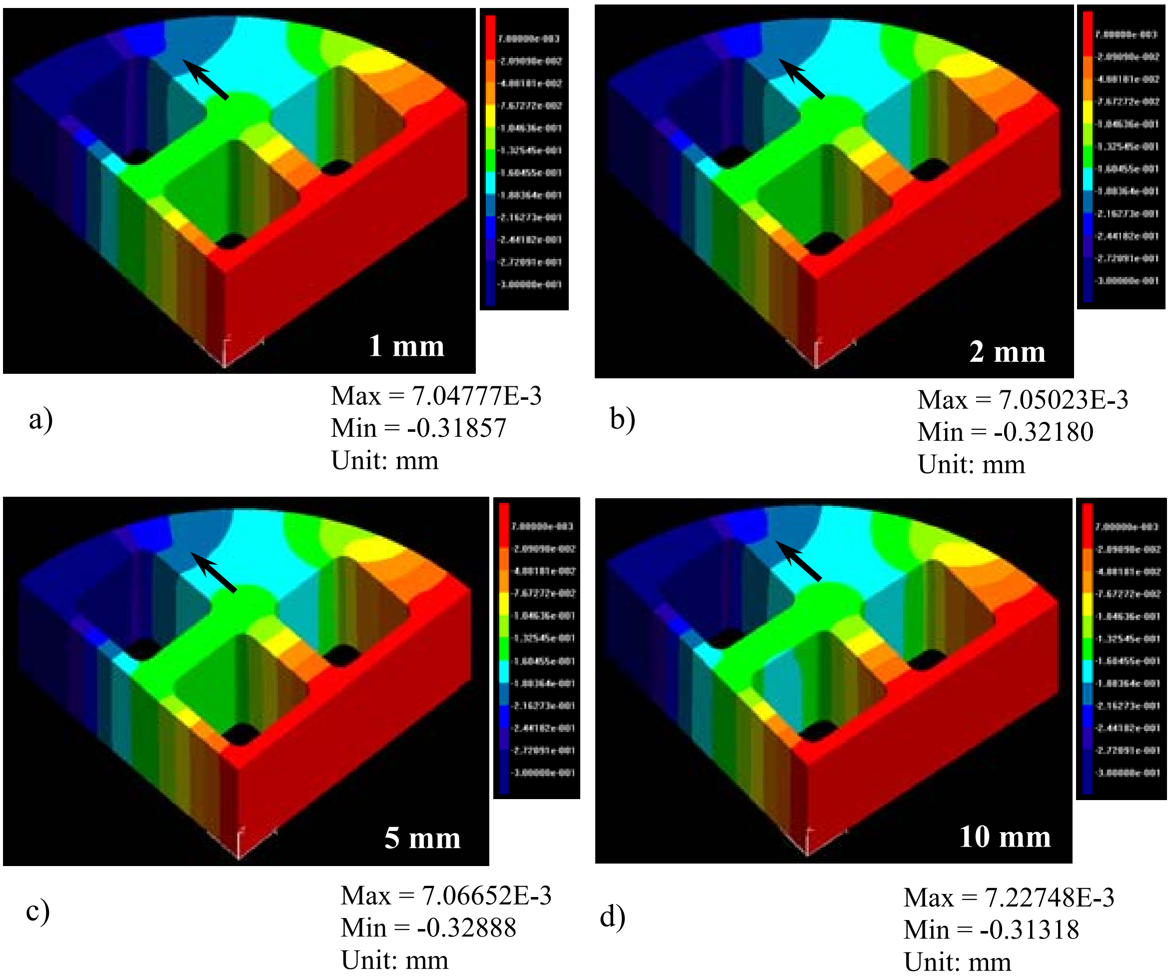

Figure 9. Displacement of BWR type canister in the *y*-direction with deciation of the fuel hole location by a) 1 mm, b) 2 mm, c) 5 mm and d) 10 mm.

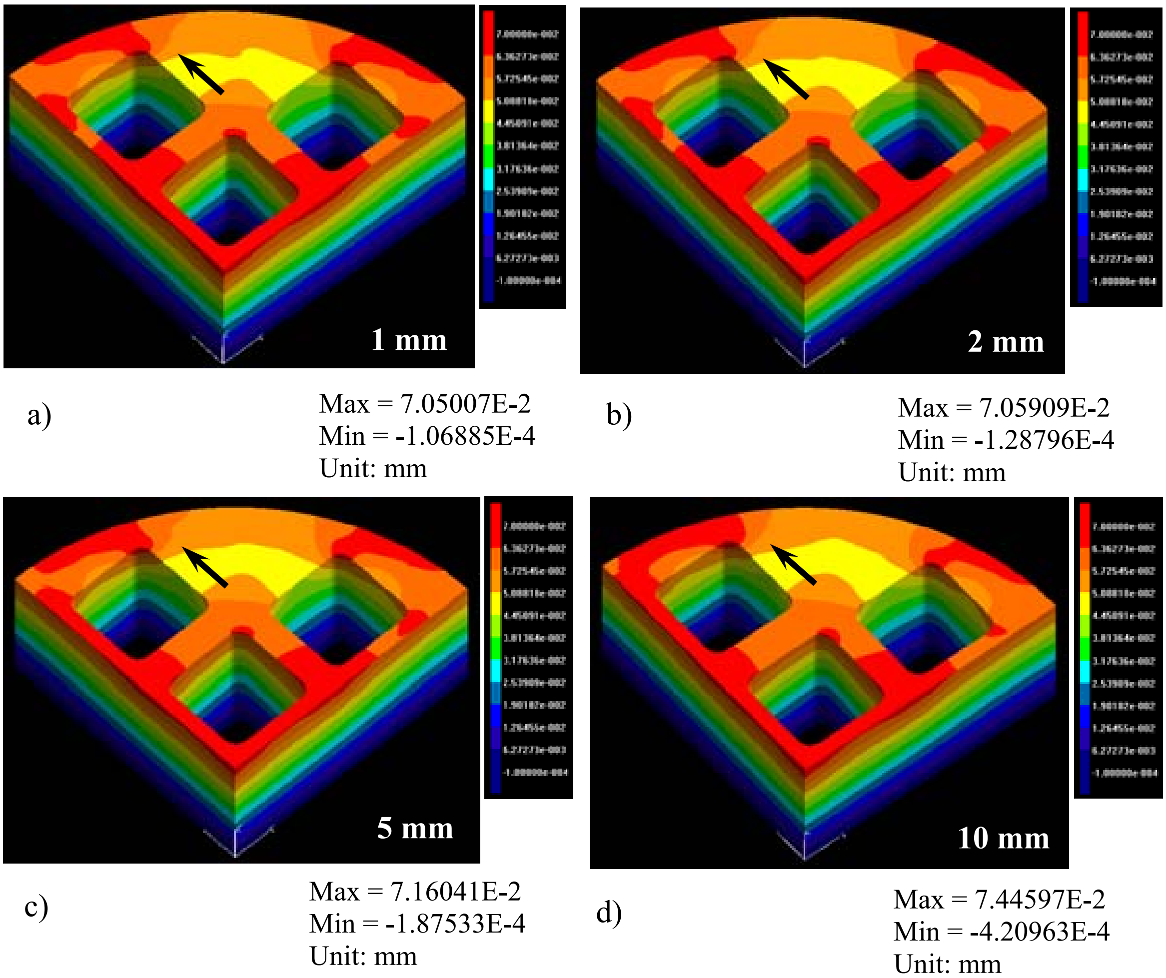

Figure 10. Displacement of BWR type canister in the *z*-direction with deviation of the fuel hole location by a) 1 mm, b) 2 mm, c) 5 mm and d) 10 mm.

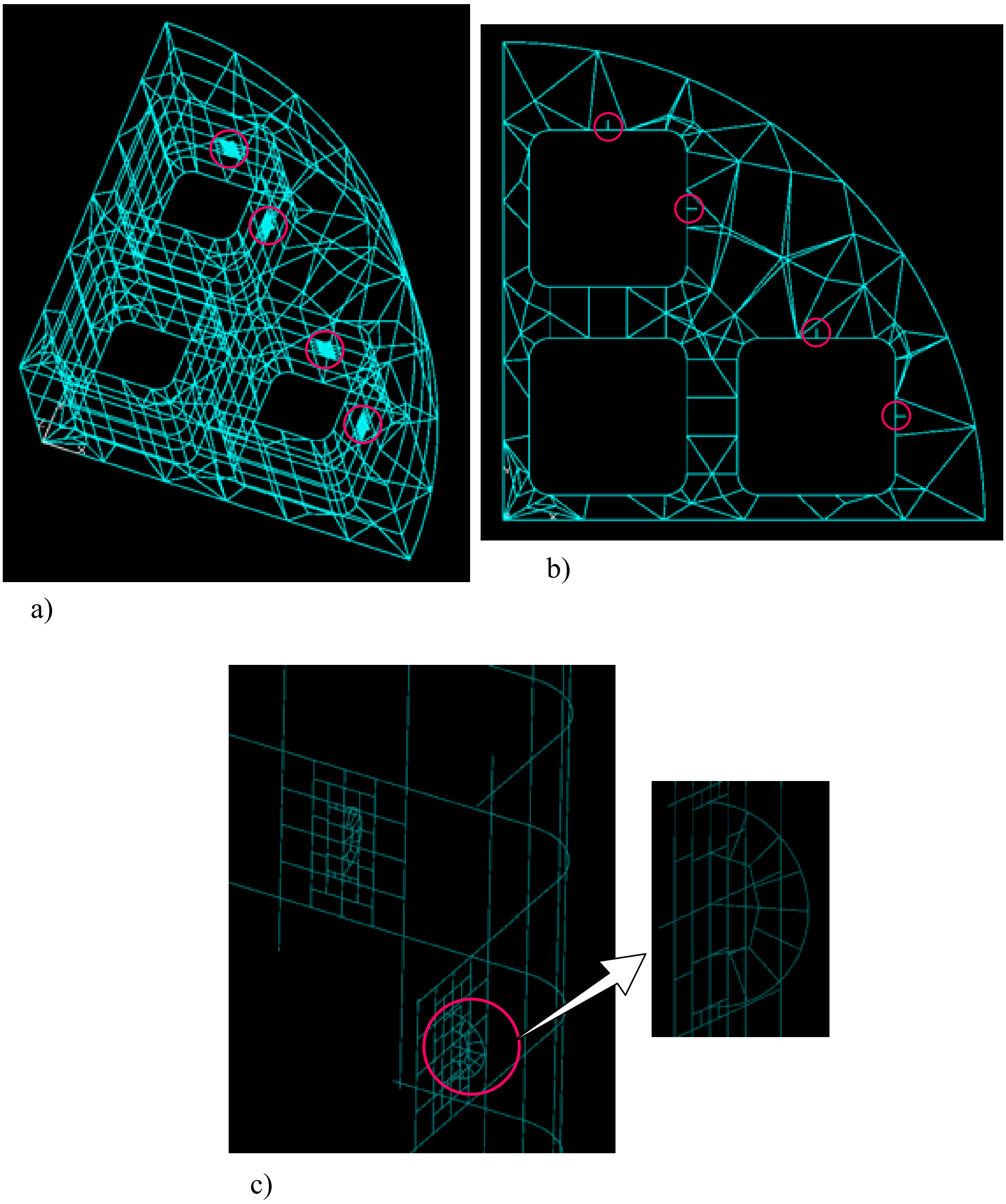

Figure 11. BEM mesh and the introduction of initial cracks at the maximum tensile stress area: a) Perspectiev view of the inserted fractures; b) Top view of the locations of the inserted initial fractures, and c) details of the fracture geometry with BEM mesh.

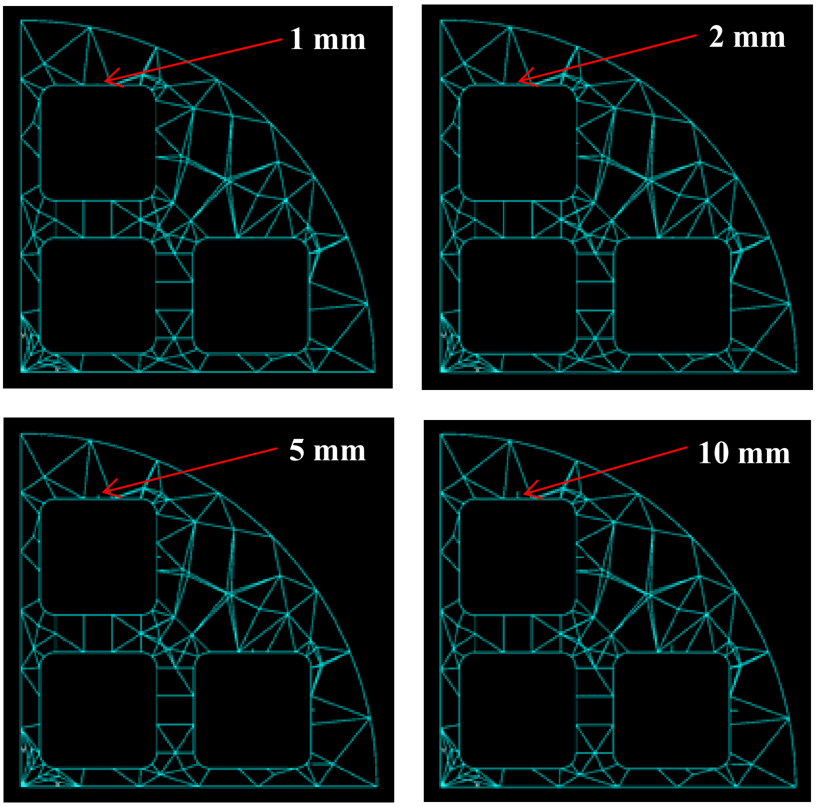

Figure 12. Top view of the initial crack with different length of 1, 2, 5, and 10 mm, respectively.

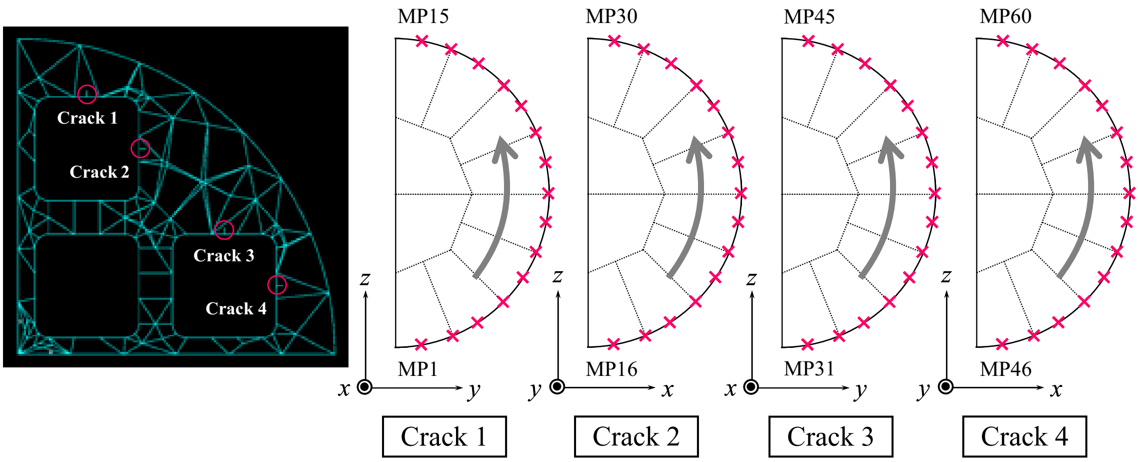

Figure 13. Locations of mesh point (MP) and their numbering convention along the tip of the inserted fracture.

4.2 Results of Loading case a)

Figure 14a illustrates the model geometry and boundary conditions for loading case a), according to Werme (1998). In order to make the model computationally possible with manageable sizes and memory requirements for 3D calculations, 1/4 symmetry was assumed so that slight changes from the original definition as in Werme (1998) is made, including the roller boundary conditions at one end of the canister. This slight change may not, however, change the stress distribution situation very much since the general distribution of the swelling pressures along the canister as described in Werme (1998) is followed.

Figures 15 and 16 show the results of loading cases a) without fracture, for maximum principal stresses (including tensile stress) and Von Mises effective stress distributions (Fig.15) and displacement (Fig.16). The maximum tensile stress can be observed at the fixed end of the canister and may, therefore, be due to boundary-end effects of numerical artefacts. More realistic tensile stresses are much smaller in magnitude (less than 25 MPa, Fig.15a) along the corner of the fuel hole. Similar situation can also be observed for distribution of the Von Mises effective stress (Fig.15b). This indicates that critical locations for fracture introduction should be along the two corners of the two fuel holes, as shown in Fig.17. The fracture size is assumed to be 1 mm, according to comparison results from loading case c).

The resultant SIF as calculated for the two initial cracks are listed in Table A21 of the Appendix. The mesh point numbers, in this case, are the actual node numbers in the model, with their locations along the fracture tipes shown in Fig. A1 of the Appendix. The calculated SIF is far smaller compared to the measured K_{IC} value so that cracks did not grow at all. The reasons for this results are the same as that for loading case c) as mentioned before.

4.3 Results of loading case b)

The loading case b) is simulated in parallel with loading case a) due to the similarity of the conceptualization of the model geometry and boundary conditions (Fig.14b), with, however, more justified symmetric conditions.

Loading case b) generated similar tensile stress and Von Mises effective stress distributions and magnitudes, as shown in Fig. 18, although with slight increase of tensile stresses at the fixed end of the canister, due to numerical boundary-end effects. Figure 19 shows the distribution of the displacements in y- and z- directions, with small magnitudes. The more realistic tensile stress area are also the two corners of the fuel holes as in laoding case a), where two fractures of 1mm in size were inserted as shown in Fig. 20. The resultant SIF as calculated for the two initial cracks are listed in Table A22 of the Appendix. The mesh point locations and numbering numbers are shown in Fig.A2 of the Appendix. Similar results were calculated for SIF, with no fracture growth observed due to the same reasons as given before.

4.4 Summary on fracture growth potentials

The simulations presented above for different loading conditions as considered in Werme (1998) and with consideration of possible fuel position deviations show that there is no risk of growth of initial fractures (due to manufacturing processes), due to the dominance of compressive stress field, high value of toughness of cast iron and low tensile stress magnitude in combination.

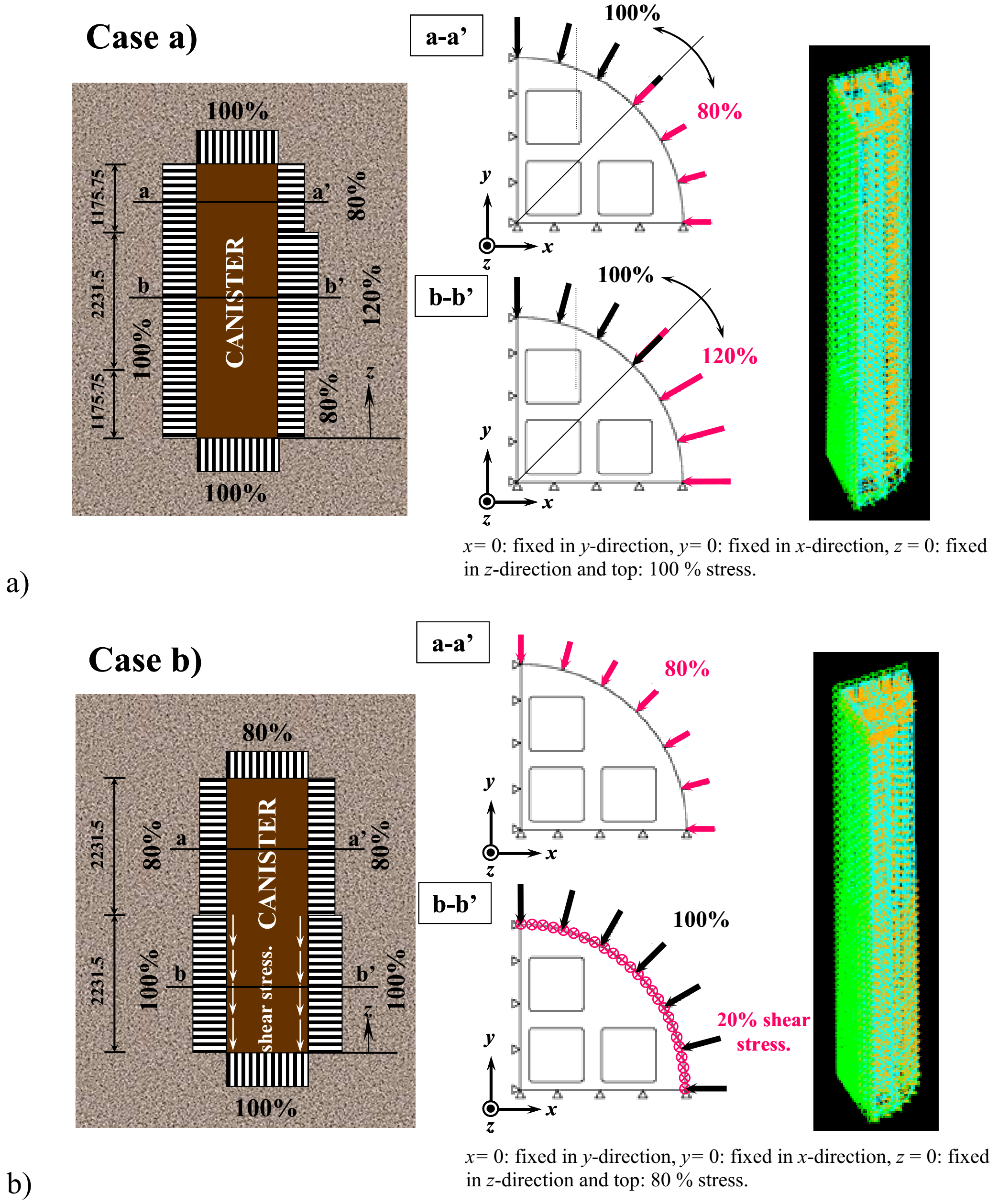

Figure 14. Two extreme loading conditions of uneven distribution of swelling pressure for full scale model based on Werme (1998) for fracture simulations. A quarter cross section of BWR type canister was used for stress calculation and fracture simulation by BEASY code. It should be noted that the stress values for 20, 80, 100 and 120 % are 8.8, 35.2, 44 and 52.8 MPa.

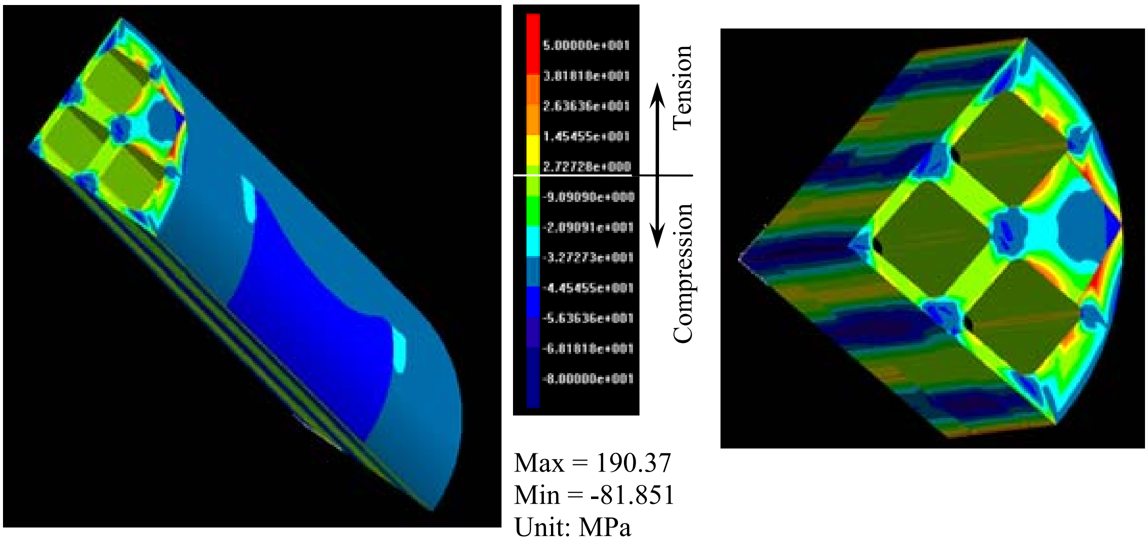

a)

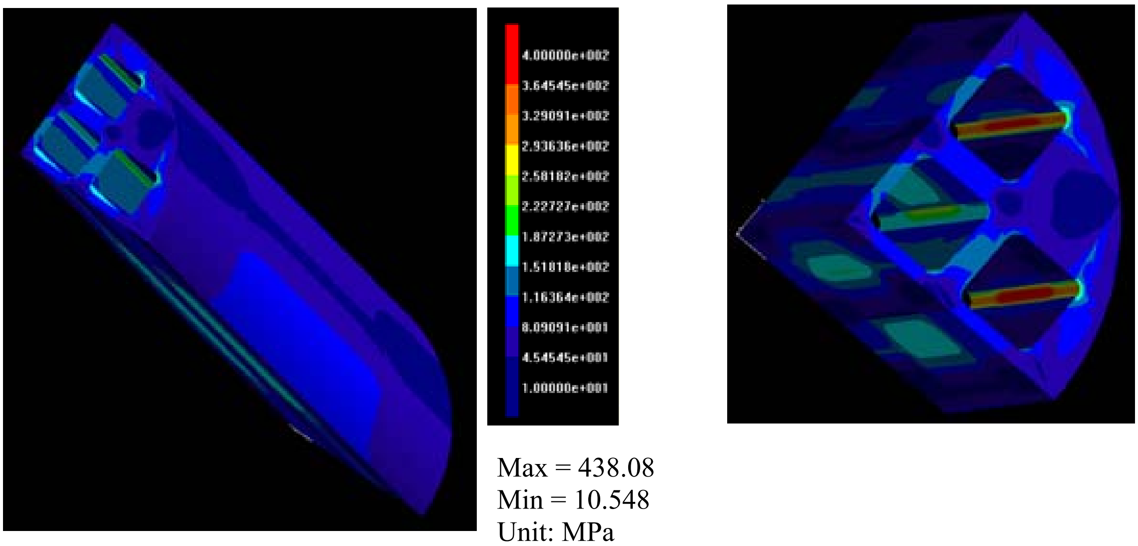

b)

Figure 15. Results of stress analysis for full scale BWR type canister with loading case a), a) Distribution of maximum principle stress (σ_1 plot) and b) Distribution of von Mises effective stress.

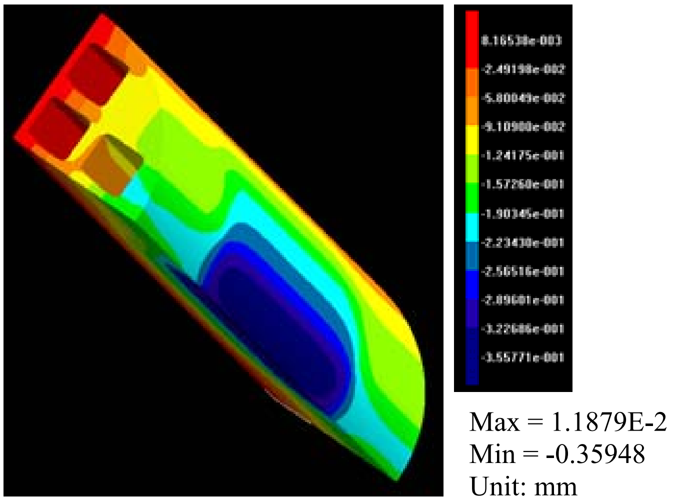

a)

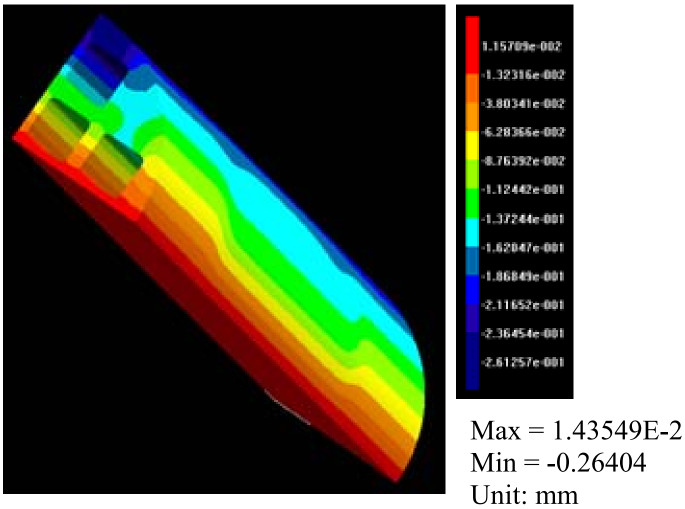

b)

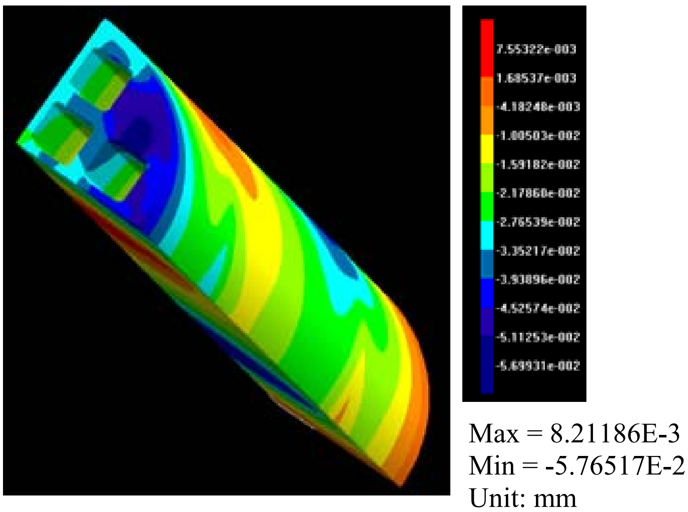

c)

Figure 16. Displacement of full scale BWR type canister with loading case a) in the a) *x*-, b) *y*-and c) *z*-direction.

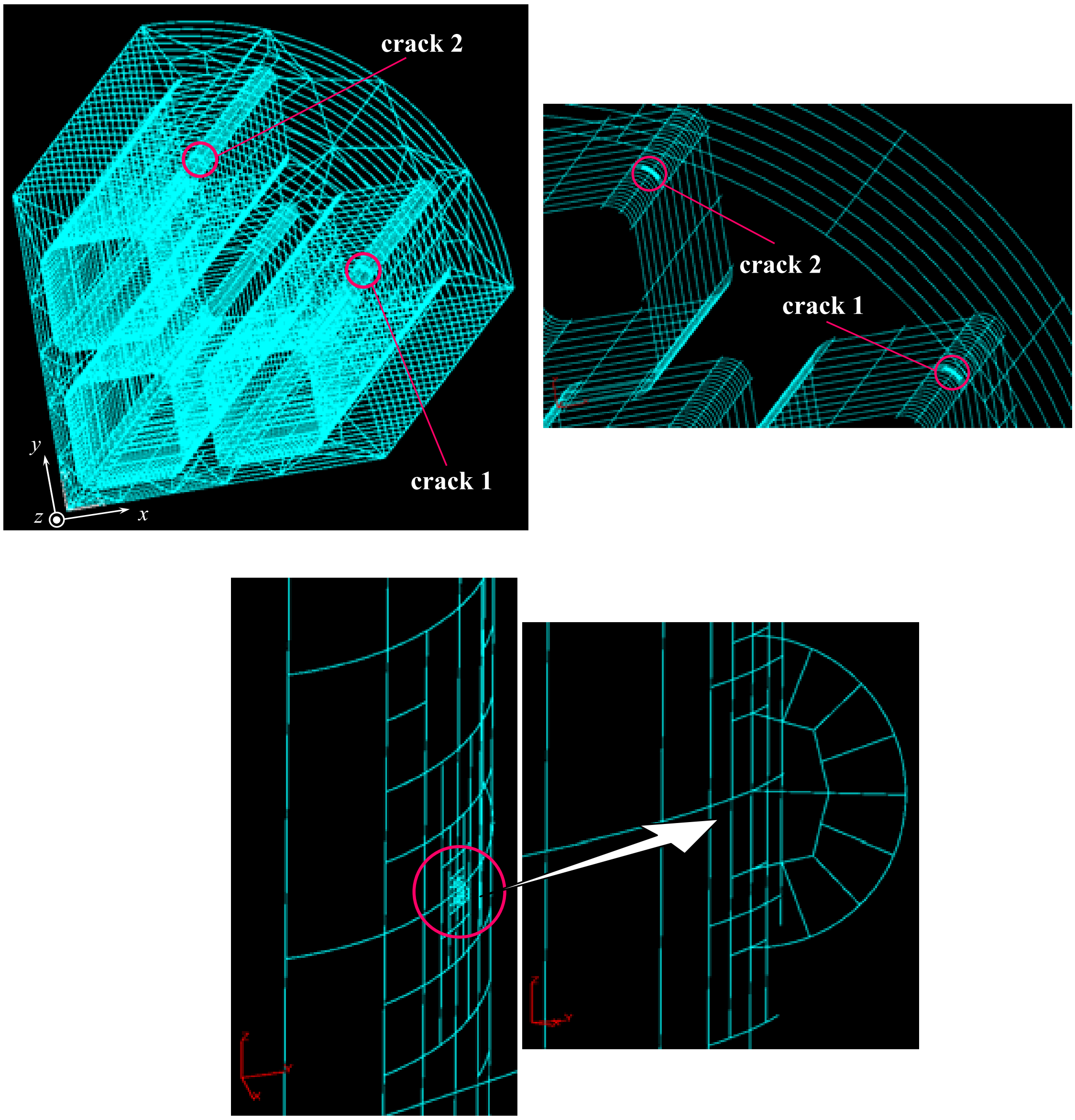

Figure 17. Introduction of two initial cracks at the maximum tensile stress area for loading case a).

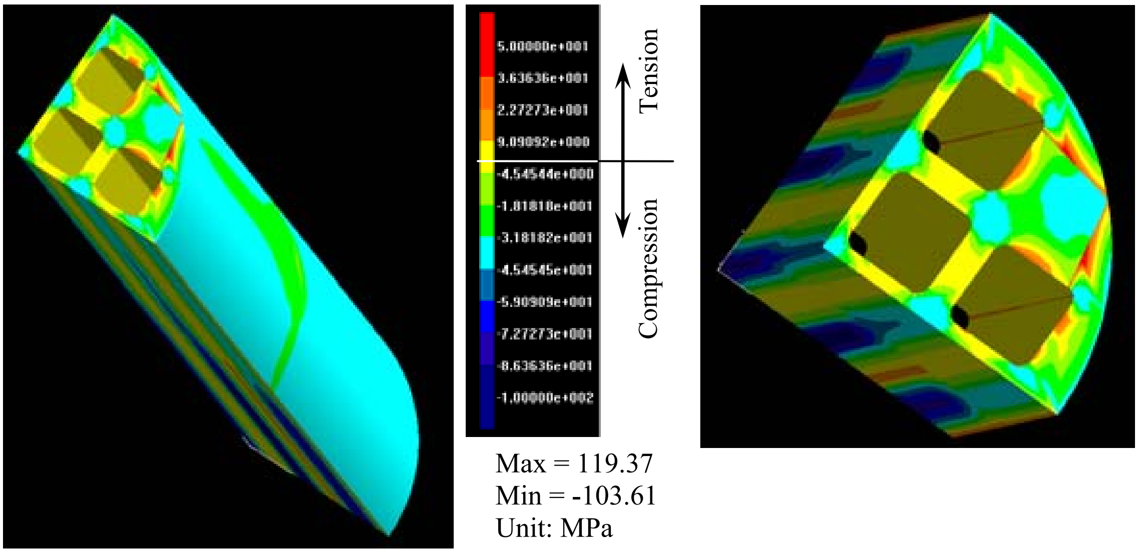

a)

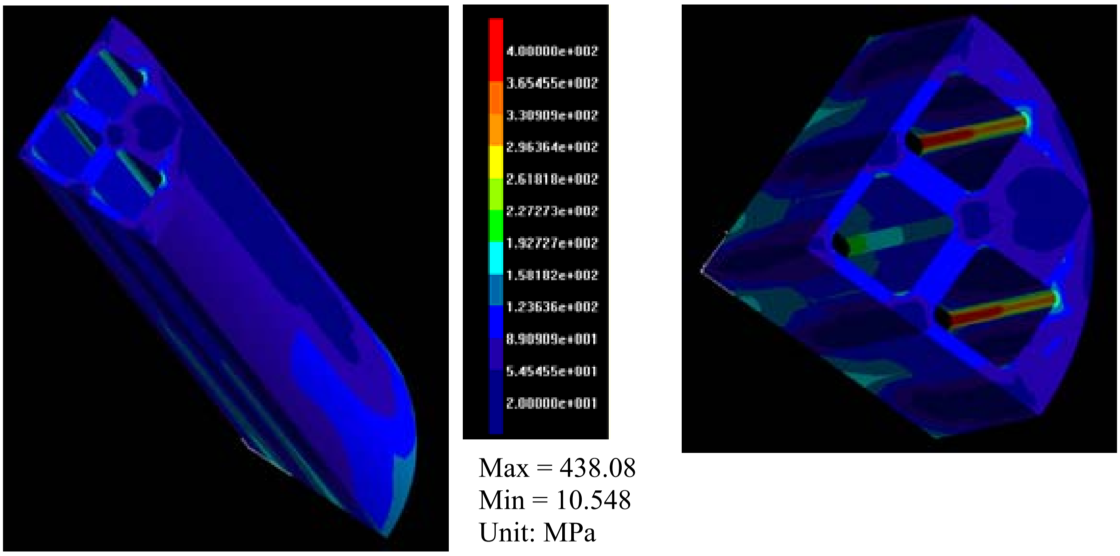

b)

Figure 18. Results of stress analysis for full scale BWR type canister with loading case b, a) Distribution of the maximum principle stress (σ_1 plot) and b) Distribution of the von Mises effective stress.

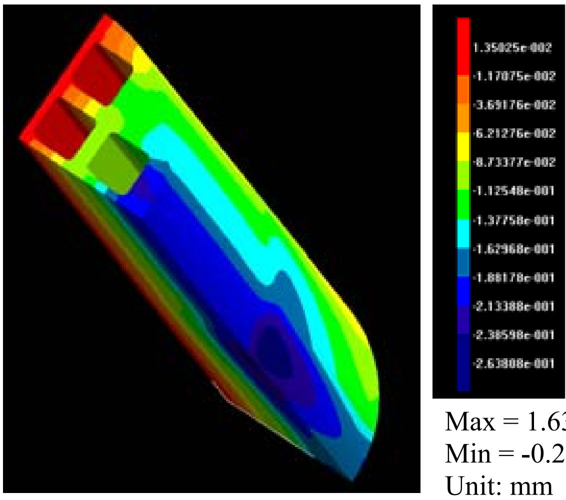

Max = 1.63322E-2
Min = -0.26664
Unit: mm

a)

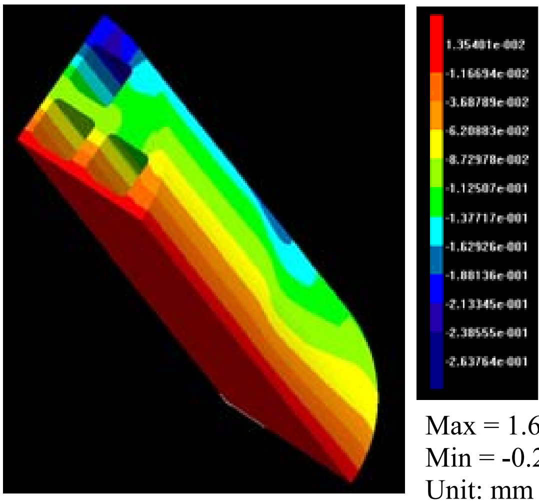

Max = 1.63698E-2
Min = -0.26659
Unit: mm

b)

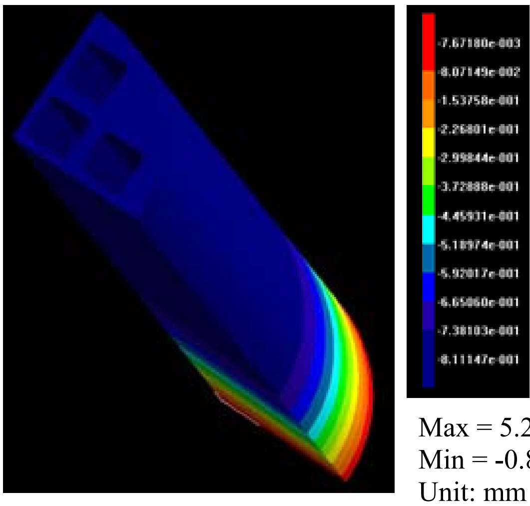

Max = 5.26918E-4
Min = -0.81935
Unit: mm

c)

Figure 19. Displacement of full scale BWR type canister with loading case b in the a) *x*-, b) *y*-and c) *z*-direction.

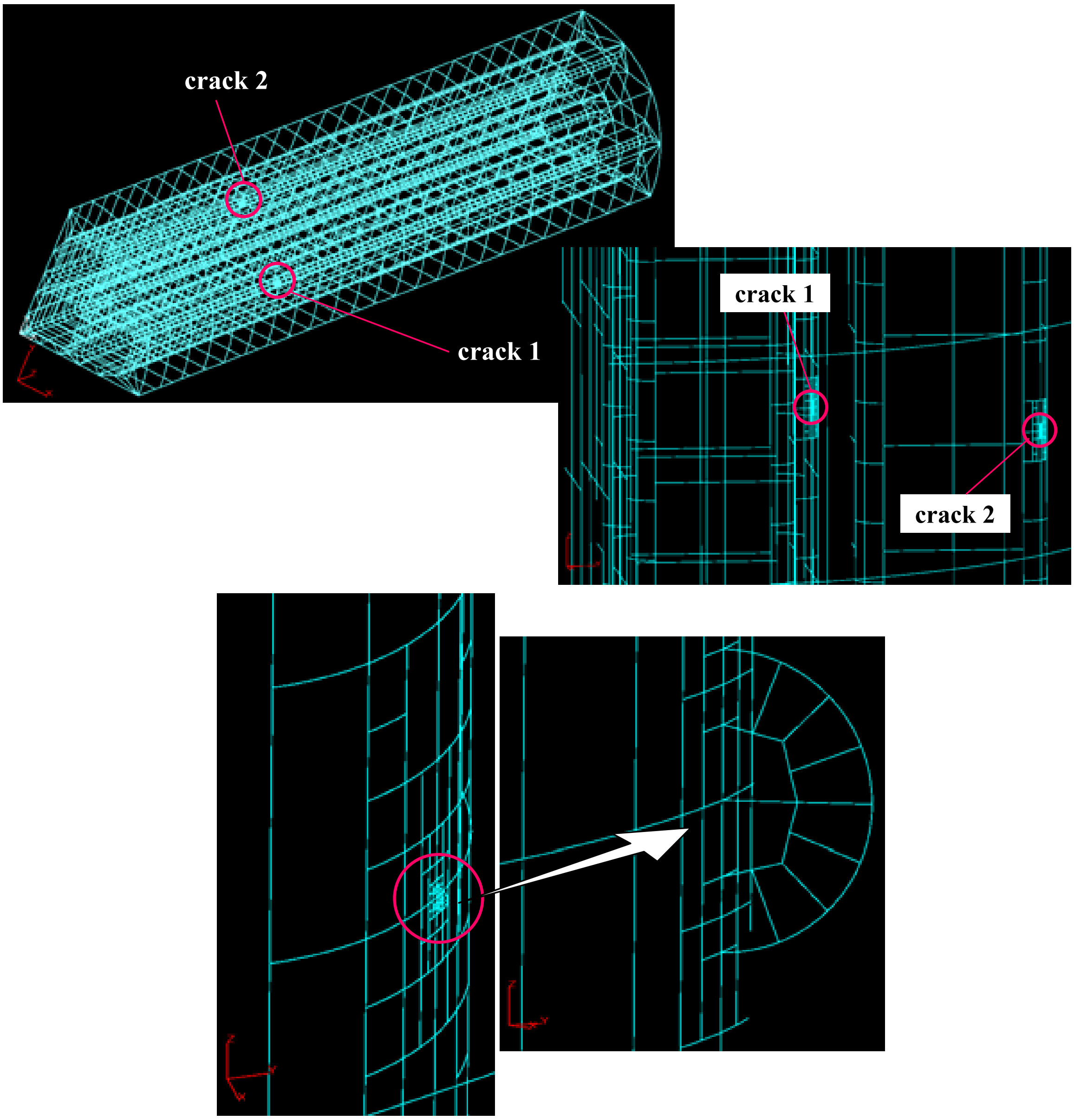

Figure 20. Introduction of initial crack at the maximum tensile stress area for loading case b.

5. RESULTS OF PLASTIC COLLAPSE OF THE CAST IRON INSERT

The plastic collapse load of the cast iron insert was simulated using a 2D FEM code ADINA. The basic concept is to gradually increase the uniformly distributed radial normal load on the outer surfaces of the insert until no more increment of load can be added without causing divergence of the solution, or buckling failure of the whole insert. Similar simulations were conduced by SKB as reported in (Dillström, 2005; Andersson et al., 2005). The objective of this FEM simulation is to re-evaluate the important issues related to this problem. In order to have a common basis of comparison with SKB works reported in (Dillström, 2005; Andersson et al, 2005), the insert geometry dimension and material constitutive model and properties used in these reports were adopted.

The ADINA code is a widely applied FEM code for structural analysis with linear elastic and non-linear elasto-plastic material models. The features of the code is well known and do not need to be repeated here. The specific code applied to this simulation, however, is a research-oriented code developed from an earlier version of the ADINA code group (Zhang, 2006), with general functionality and a library suite of constitutive models for structural analysis with elastic and elasto-plastic behaviours.

5.1. Geometry mode

Due to the symmetry in both insert geometry and boundary conditions, only 1/8 of the insert needed to be included in the finite element model. The resulting finite element model is shown in Figure 21, using outer radius = 474.5 mm and the corner radius = 20 mm, respectively.

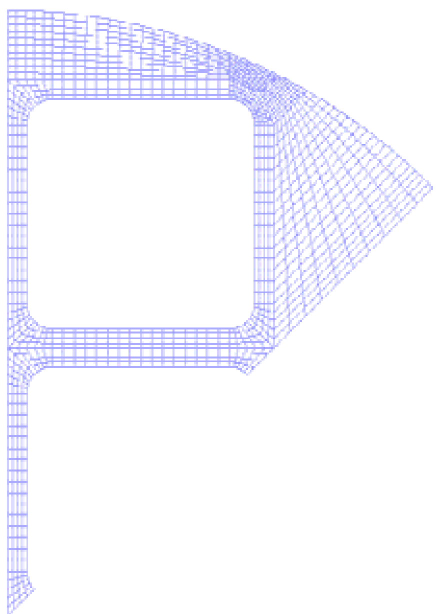

Figure 21. Finite element model used for loading case d) for plastic collapse analysis.

5.2. Material Properties

The calculations were made using a simplified multilinear elastic-plastic material model for the cast iron. The stress-strain curve of the material is defined as piecewise linear in the strain-stress space, based on on a Von Mises yield surface and an associated flow rule, with isotropic multilinear hardening. The material properties used include: Young's modulus $E = 160000\text{N/mm}^2$, Poisson's ratio $= \nu = 0.286$, yield stress $R_{0.2} = 270\text{N/mm}^2$, strain at $R_{0.2}$ ($\varepsilon_{sy} = R_{0.2} / E$)=0.0016875, respectively. The other parameters are: at strain $\varepsilon_{su1} = 0.1$ the ultimate strength $R_{m1} = 480\text{N/mm}^2$; at strain $\varepsilon_{su2} = 0.3$ the ultimate strength $R_{m2} = 580\text{N/mm}^2$, respectively.

5.3. Analysis results

5.3.1 Stresses and stress concentrations

Figures 22-29 present the distributions of the Von Mises effective stress with the normal load (*p*) at outer surfaces equal to 15, 25, 35, 45, 60, 65 and 75 MPa, respectively. These figures demonstrate the evolution of stress concentration areas during increasing pressure at the outer surface of the cast iron insert. These areas of stress concentration starts at the upper right corner of the fuel holes closest to the outer wall (Fig.22), then spread in the walls, especially the separation parts between the fuel holes (Figs. 23-28). The changes in the geometry when the outer pressure reaches 75 MPa are shown in Figs. 29 and 30 at enlarged scales. Tensile stresses of small magnitudes appears then at the outer surface and inner wall surfaces (the red crosses in the stress vector plot of Fig.31), as also predicted by the BEM models presented in Chapter 4. Figures 32-35 show the distributions of the maximum principal stress σ_1 with increase of the pressure on the outer surface.

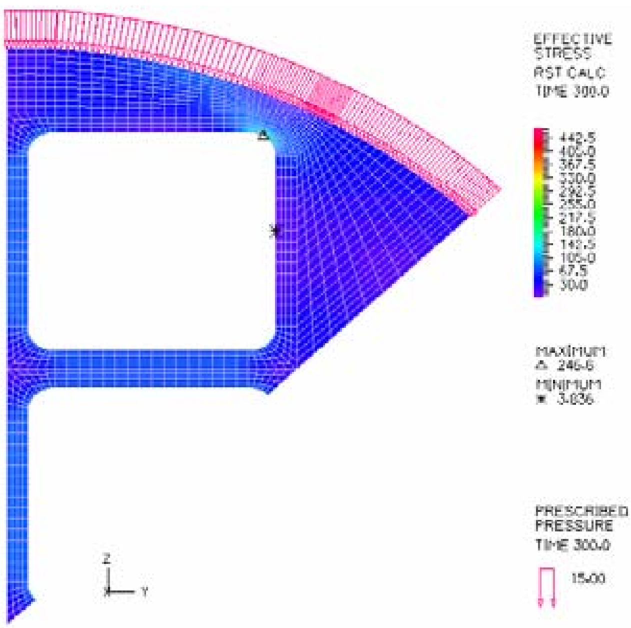

Figure 22. Von Mises effective stresses when *p* = 15 MPa.

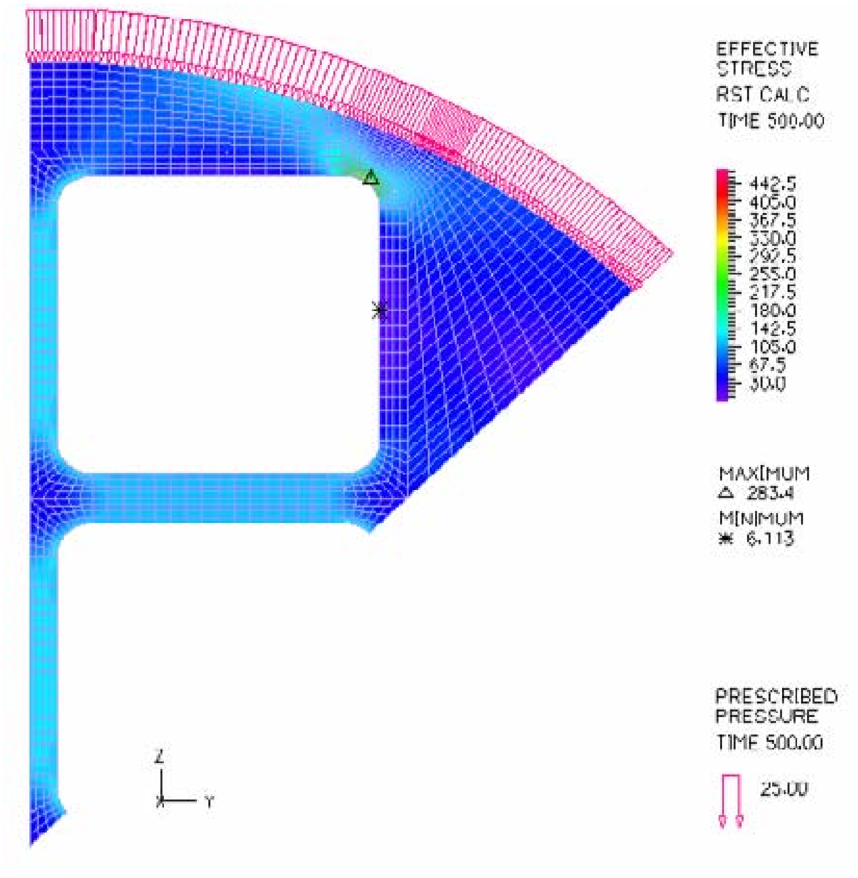

Figure 23. Von Mises effective stresses when $p = 25$ MPa.

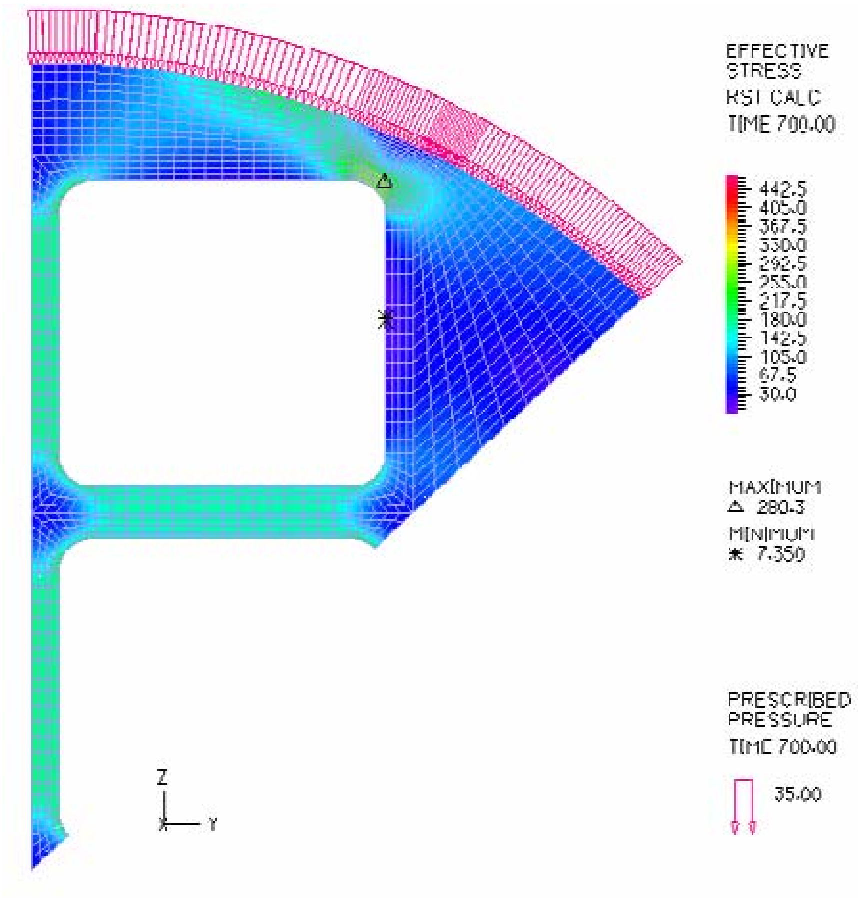

Figure 24. Von Mises effective stresses when $p = 35$ MPa.

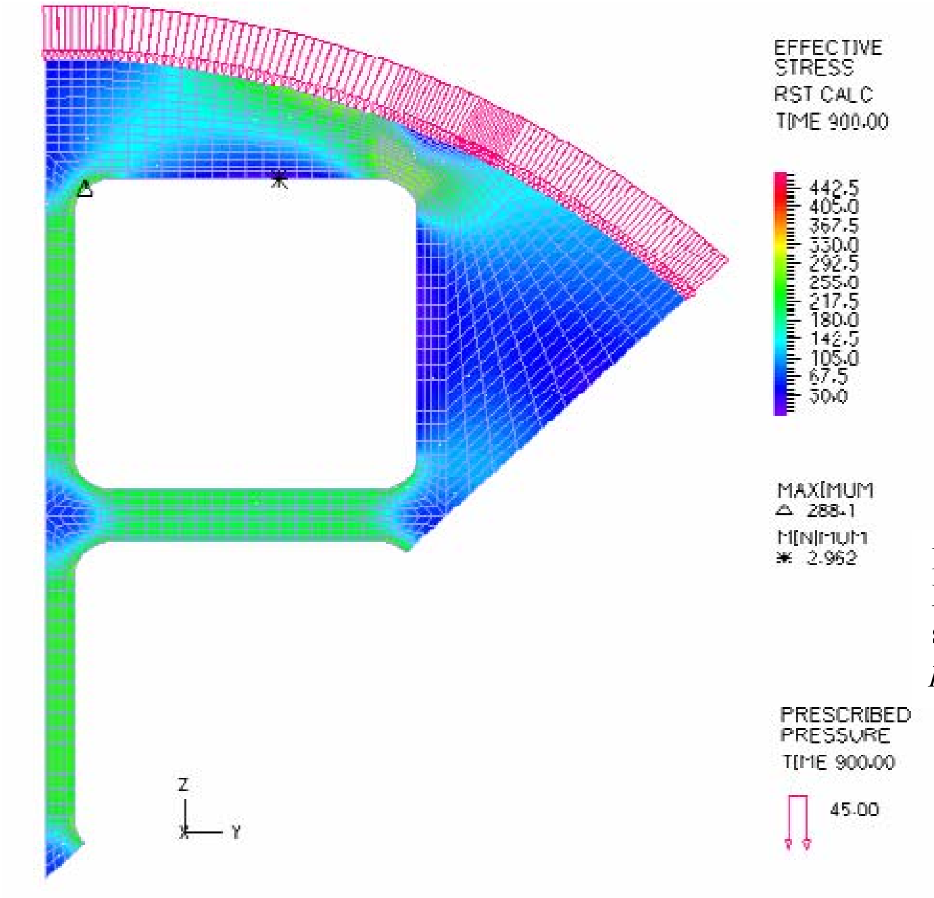

Figure 25. Von Mises effective stresses when p = 45 MPa.

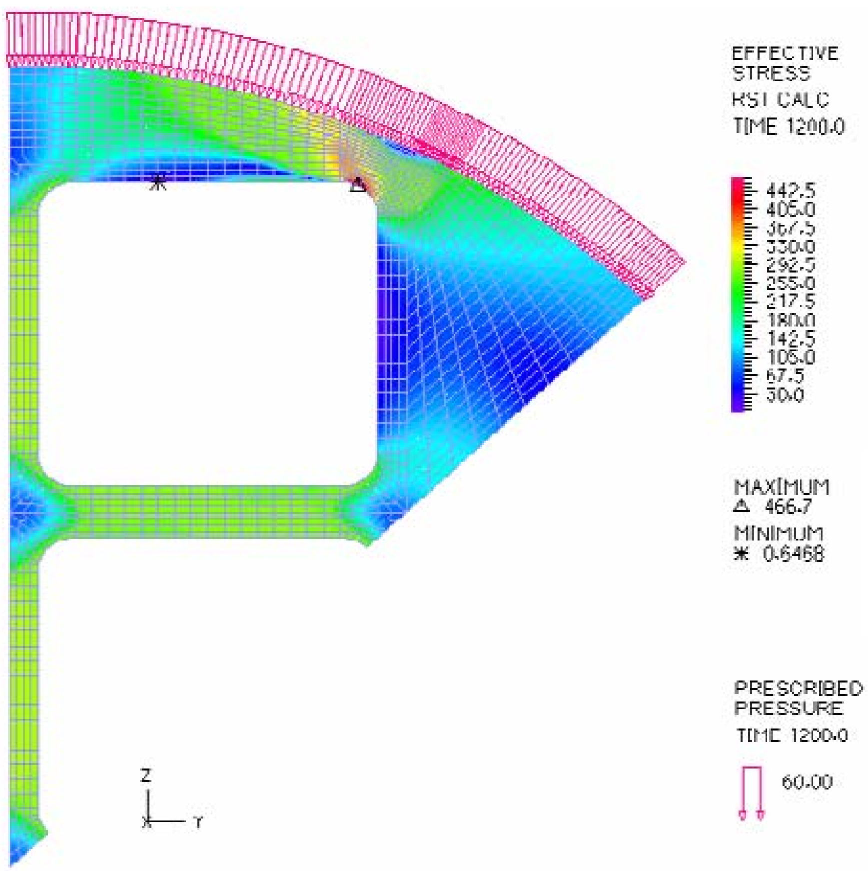

Figure 26. Von Mises effective stresses when p = 60 MPa.

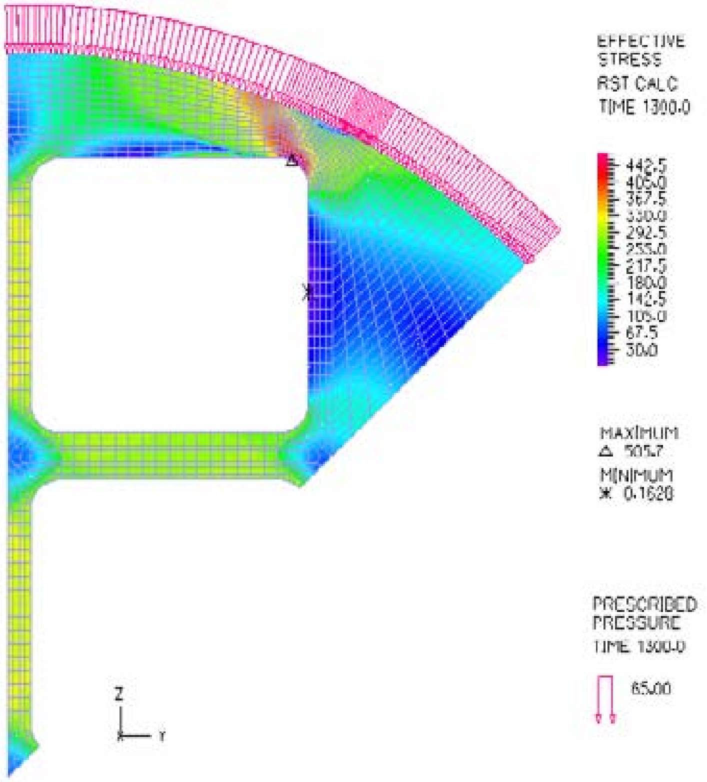

Figure 27. Von Mises effective stresses when $p = 65$ MPa.

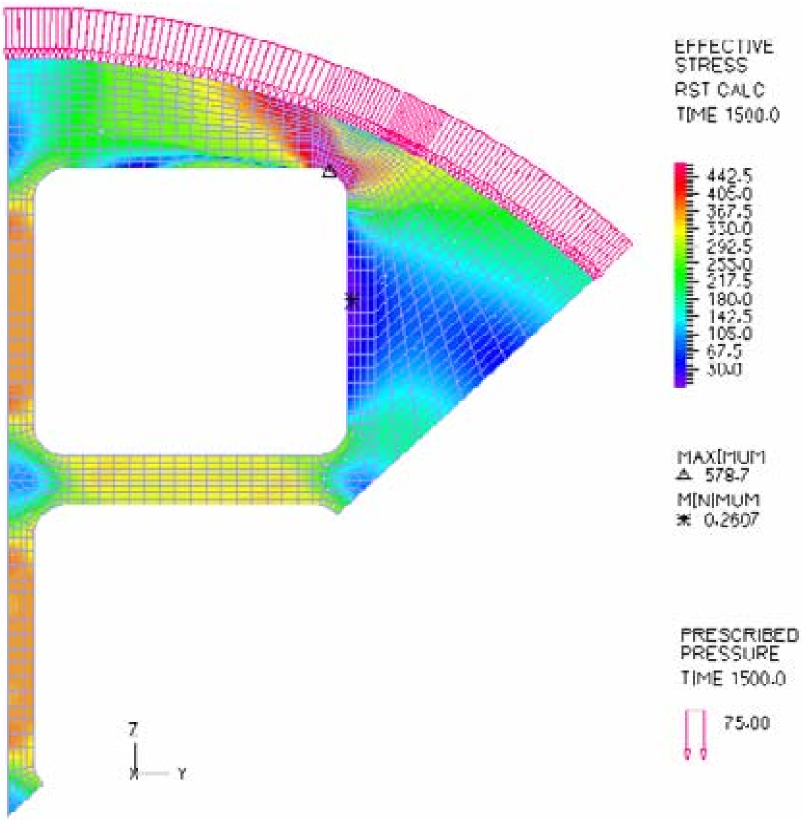

Figure 28. Von Mises Effective stresses when $p = 75$ MPa.

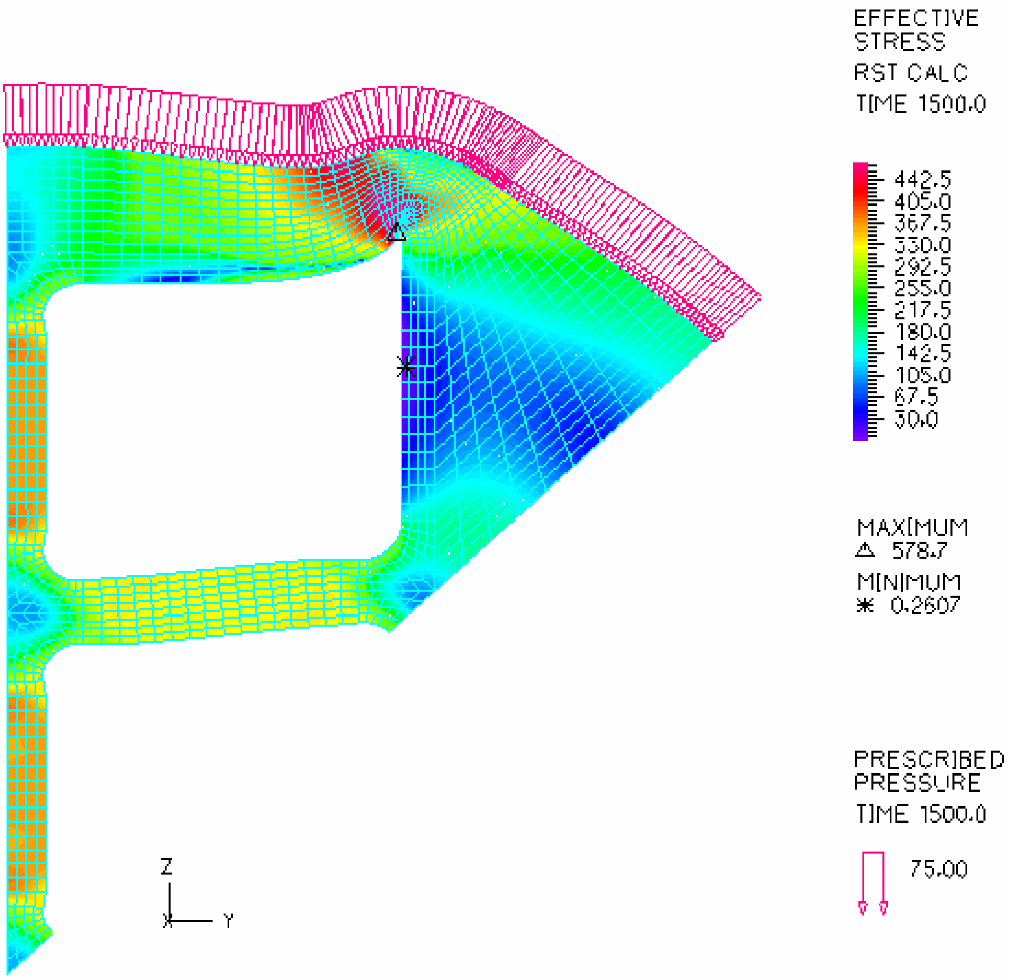

Figure 29. Final collapse geometry (collapse analysis using ADINA), plot of the effective stress at the final collapse pressure = 75 MPa.

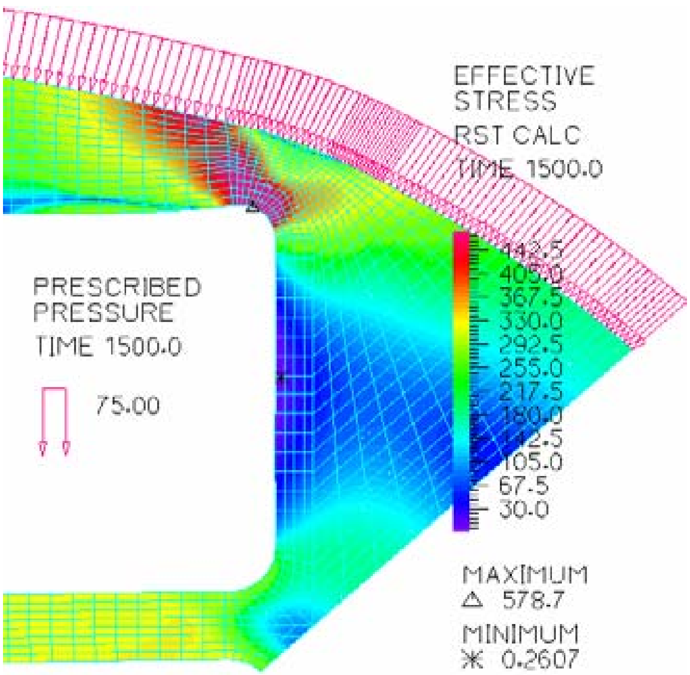

Figure 30. Effective stresses close to the corner radius when p = 75MPa.

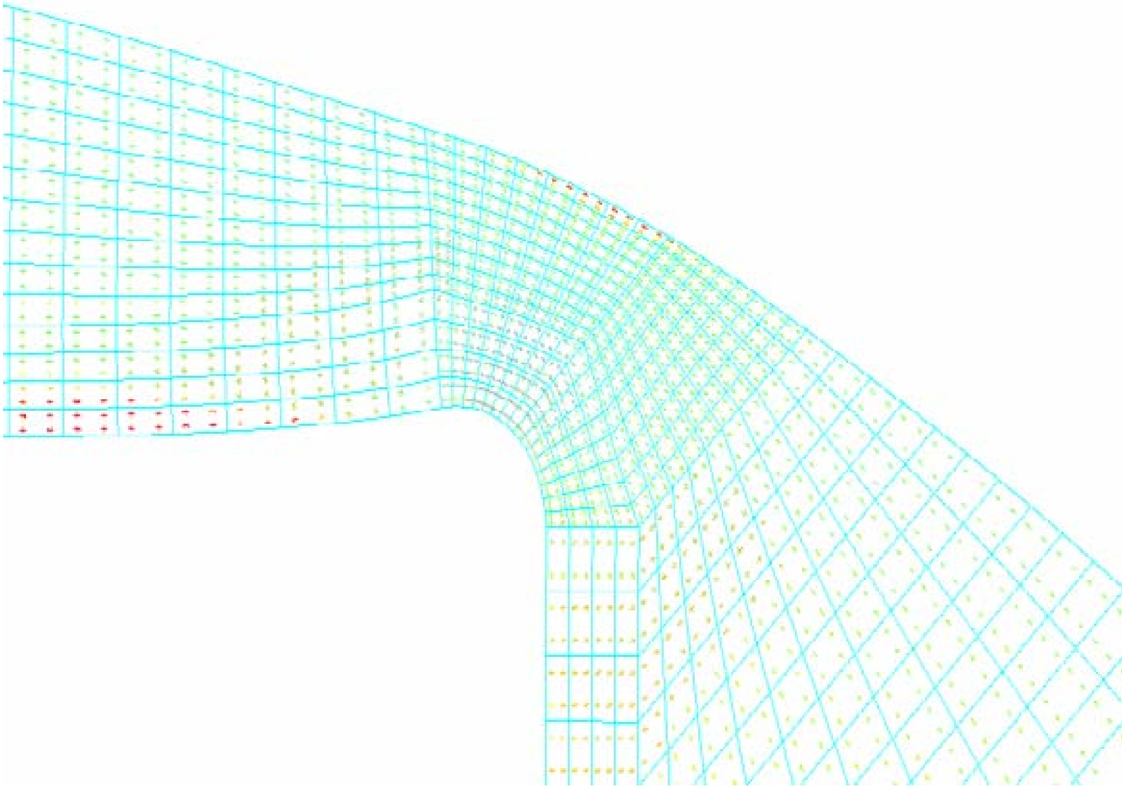

Figure 31. Principal stresse vectors close to the upper right corner of the fule hole closest to the outer surface of the insert. The red crosses indicate tensile stresses.

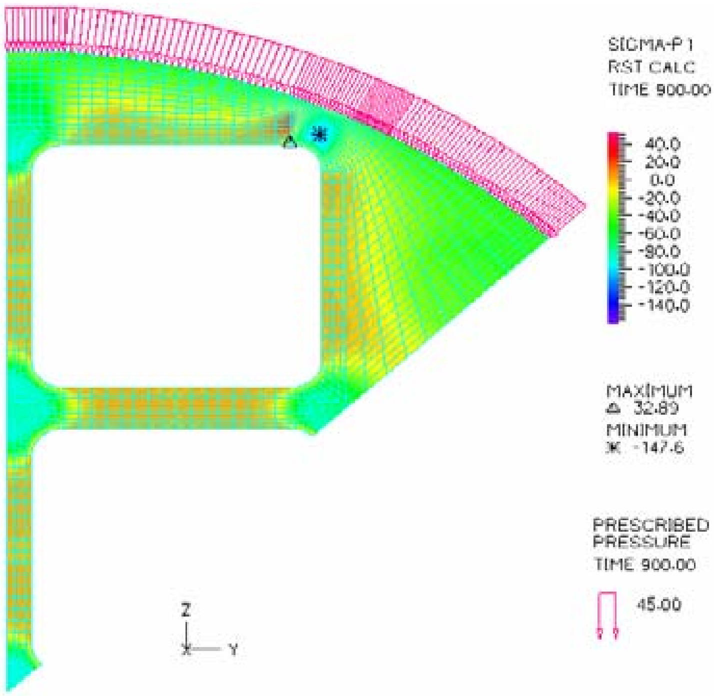

Figure 32. Principal stress (σ_1) when p = 45 MPa.

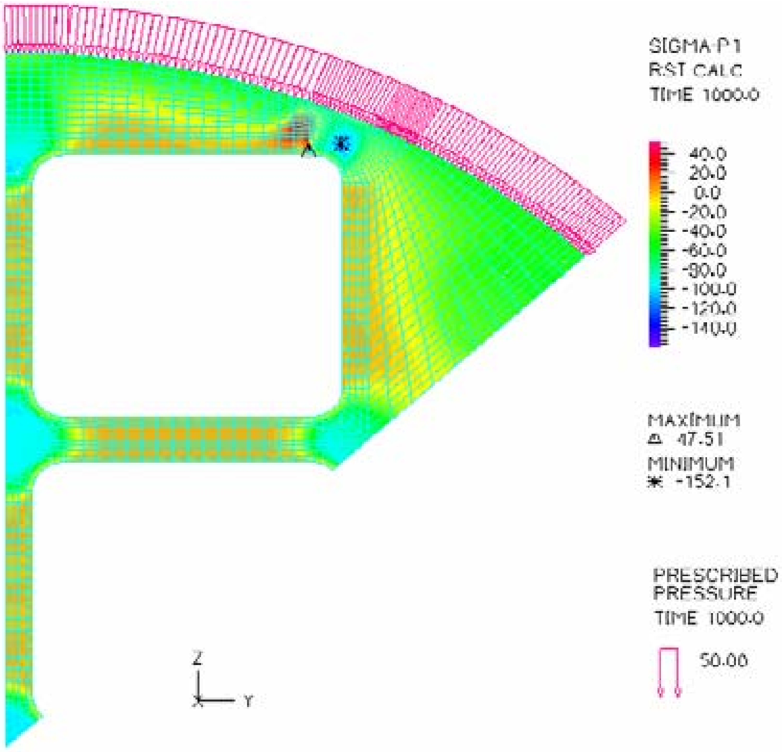

Figure 33. Principal stress (σ_1) when p = 50 MPa.

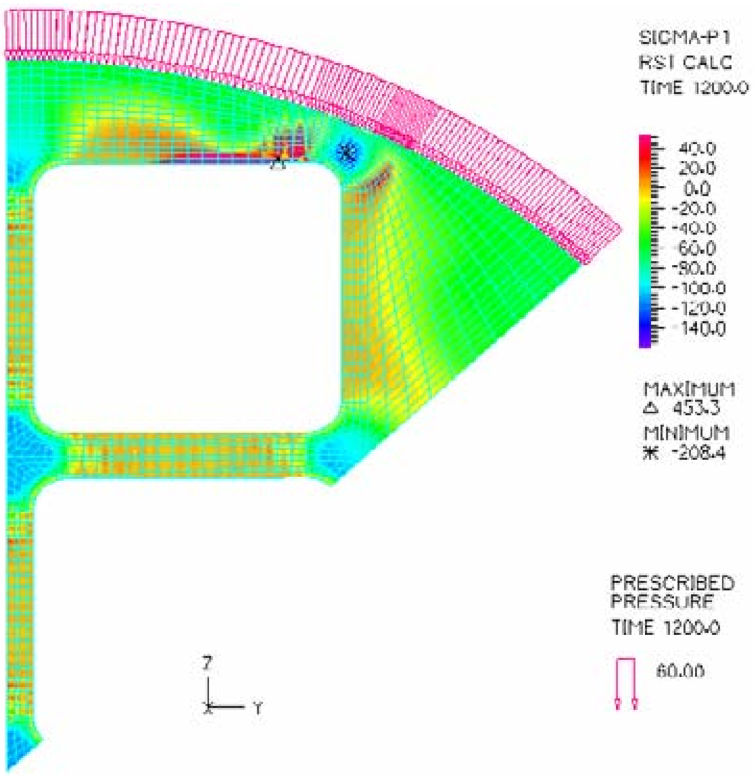

Figure 34. Principal stress (σ_1) when p = 60 MPa.

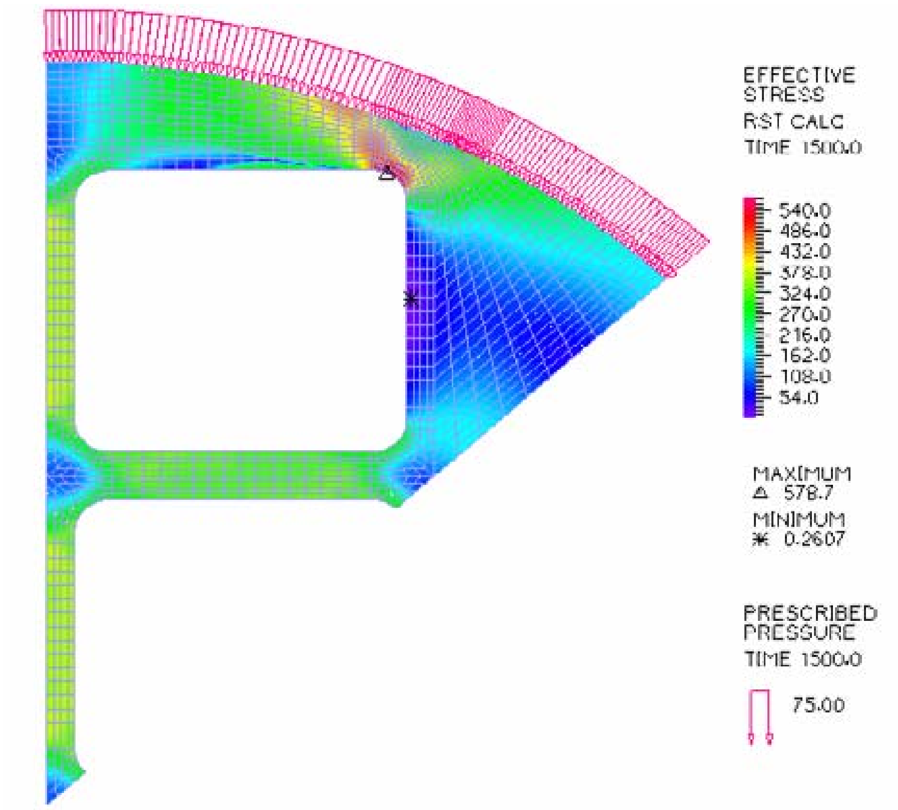

Figure 35. Principal stress (σ_1) when p = 75 MPa

In all cases the stress state of the insert was mainly compressive. When the external pressure is below ~ 30 MPa a stress concentration (in compression) dominates the stress field at the fuel channel closest to the outside surface of the insert.

As already stated above, the stress state of the insert was mainly compressive, but there was also a region with tensile stresses at the fuel channel facing the outside of the insert (see Figs. 32-35). The size of the region with tensile stresses increased with the applied pressure and also increased as the corner radius became smaller or as the fuel hole eccentricity became larger. The stress component that is most interesting, regarding initiation of crack growth, is related to the principal stress (σ_1) if in tension. The largest principal stress in tension is located within the material (when the external pressure is below ~ 45 MPa, Figs. 31 and 32) or at the inner surface (when the external pressure is above ~ 45 MPa, Figs. 33-35), which is of the similar magnitude and location as calculated by the 3D BEM BEASY models presented above. However, their magnitude is not large enough to creat new fractures.

5.3.2 Plastic strain (flow)

The plastic strain (flow) is the main variable for evaluating the stability of the insert. As the external pressure increases, also the plastic strain (flow) increases until a local collapse of the ligament occurs, as shown in Figs. 36-39. The plastic strain concentrates around the upper right corner of the fule hole closes to the outer surface of the insert and starts near the corner with a small area (Fig. 36). With increasing external pressure, the concentration area increases from the corner outwards to the outer surface, when the external pressure is no more than 55 MPa (Fig. 37). Beyond this pressure, not only the plastic flow concentration near the corner grows further and reaches the outer surface, but also occurs in one of the ligaments (separating the fuel holes), Fig. 38. At the external pressure = 75 MPa, Fig. 39, a large plastic strain area connecting the corner and the outer surface of the insert is created, and all ligaments of the fuel holes are under plastic strain (flow) conditions. This indicates that a plastic collapse will occur. In the FEM simulations, at p = 75 MPa, convergence of plastic strain calculation cannot be maintained with the built-in plastic strain iteration algorithm, indicating the structure is close to final collapse.

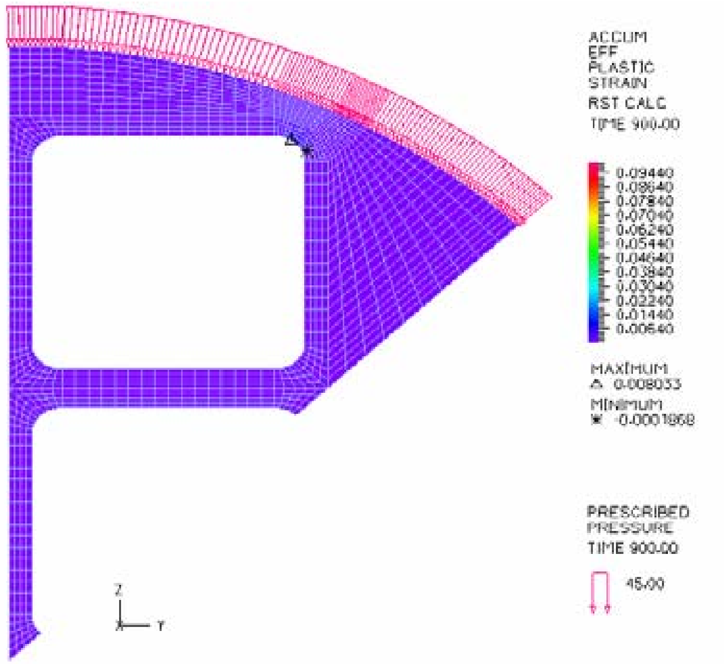

Figure 36. Effective plastic strains when p = 45 MPa.

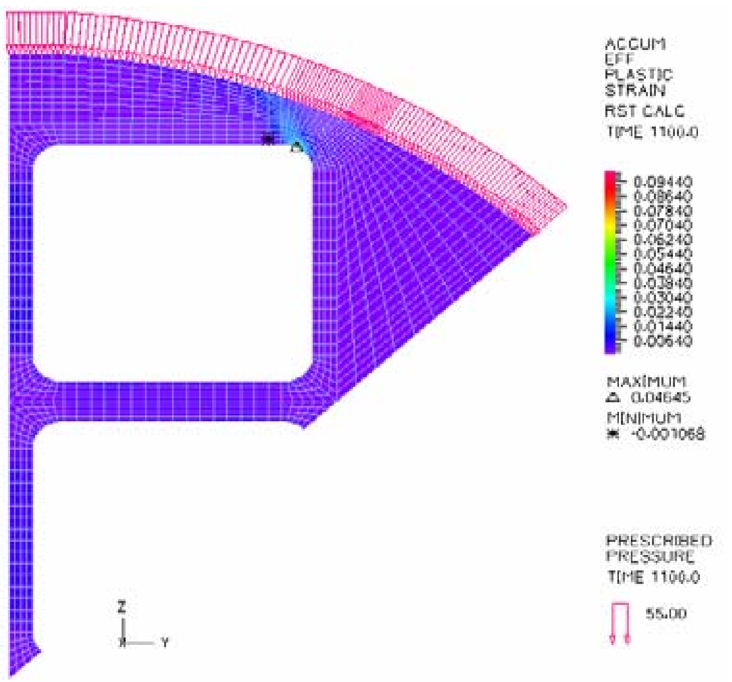

Figure 37. Effective plastic strains when p = 55 MPa.

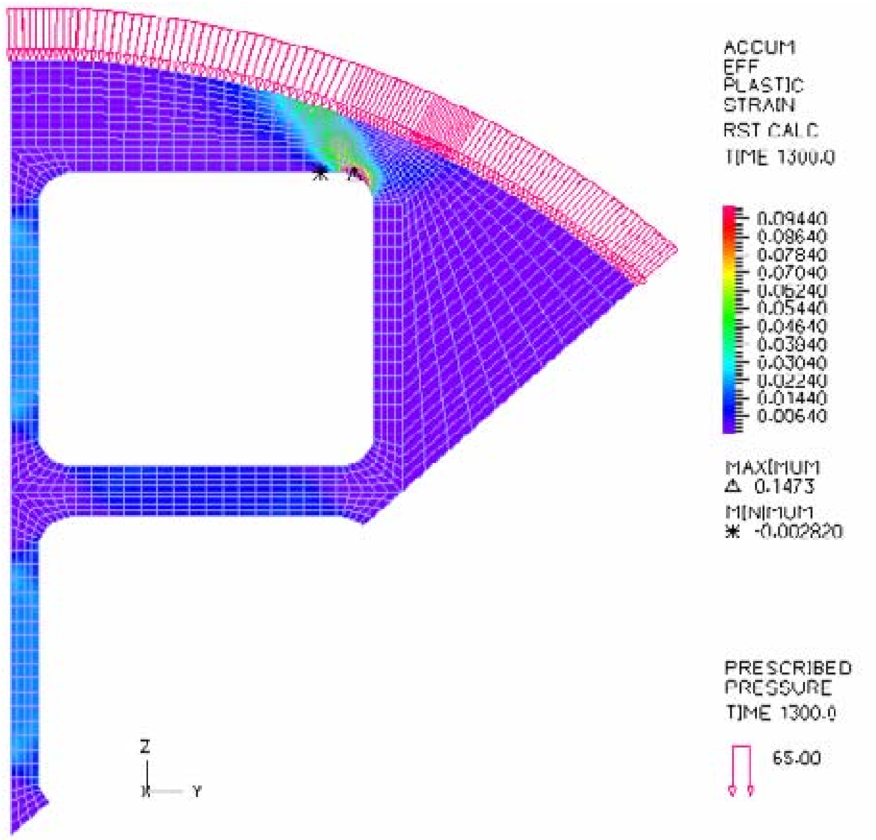

Figure 38. Effective plastic strains when p = 65 MPa.

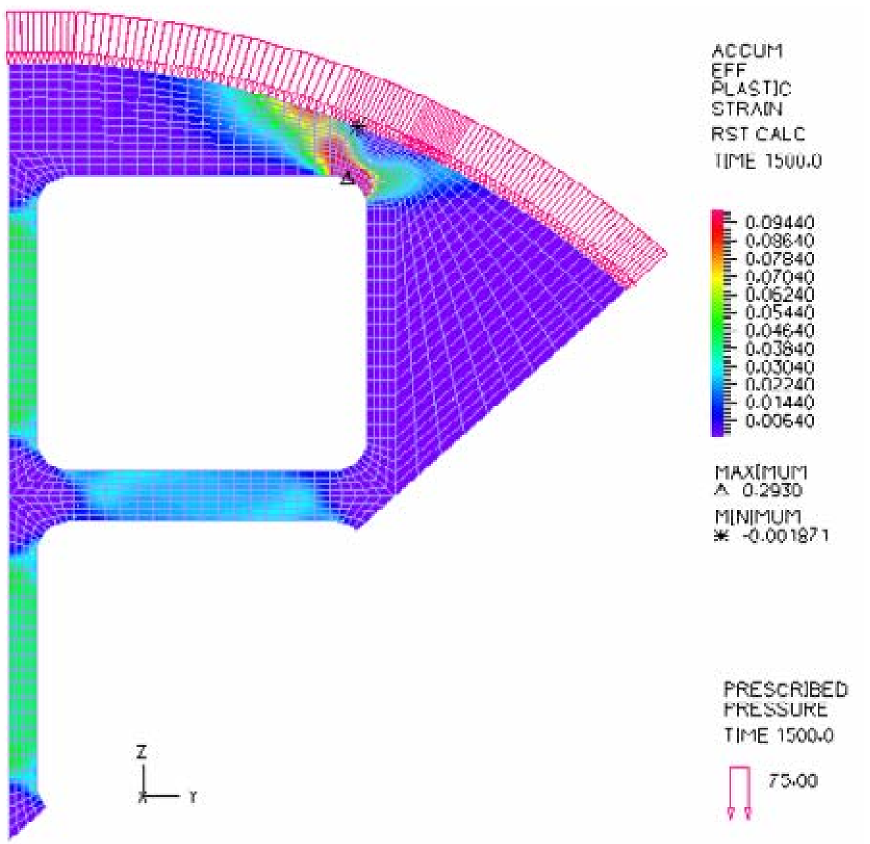

Figure 39. Effective plastic strains when p = 75 MPa.

It should be noted that the total collapse of the insert is determined not only by the formation of plastic flow region between the corner and outer surface, but also, or even more importantly, determined by the plastic states of the ligaments. Structal stability of the insert can be lost only when all ligaments enter the plastic flow state. This state is achieved at outer external pressure of 75 MPa as indicated in Fig.39.

The external pressure of 75 MPa is therefore defined as the final plastic collapse load of the insert. However, this only indicate the start of total collapse, not necessarily the absolute final collapse load since serious buckling failure of the ligaments have not occurred. More load can still be added to produce total buckling failure of the ligaments, which cannot be performed by the current FEM code.

Figure 40 show the external pressure and displacement in the z-direction in one of the ligament. It can be seen that the insert deforms elastically until the external pressure reaches a magnitude of 50 MPa. Beyond this pressure, the insert deformed plastically. The calculation has to be stopped when the external pressure is beyond 75 MPa because convergence of the plastic simulations can no longer be achieved.

The above results are also similar to tha reported in (Dillström, 2005) qualitatively in terms of stress magnitude, and distributions, and the patterns of plastic strain distributions. The final collapse load of 75 MPa is, however, smaller that that estimated in Dillström (2005). The most probable reason, as mentioned above, is the resolution requirements for iterations during the plastic strain calculation using the return-map algorithm to project the overestimated strain onto the yield function surface. The ADINA code applied in this analysis set a quite strict convergence criterion so more significant plastic flow generated by higher loading force cannot meet the convergence criterion. The commercial code applied in the calculations in Dillström (2005) may have more advanced plastic strain calculations for maintaining convergence of results with large plastic deformations so that larger collapse load may be obtained. Another reason, but perhaps a minor one, is the difference in the FEM models, such as mesh resolution and distribution.

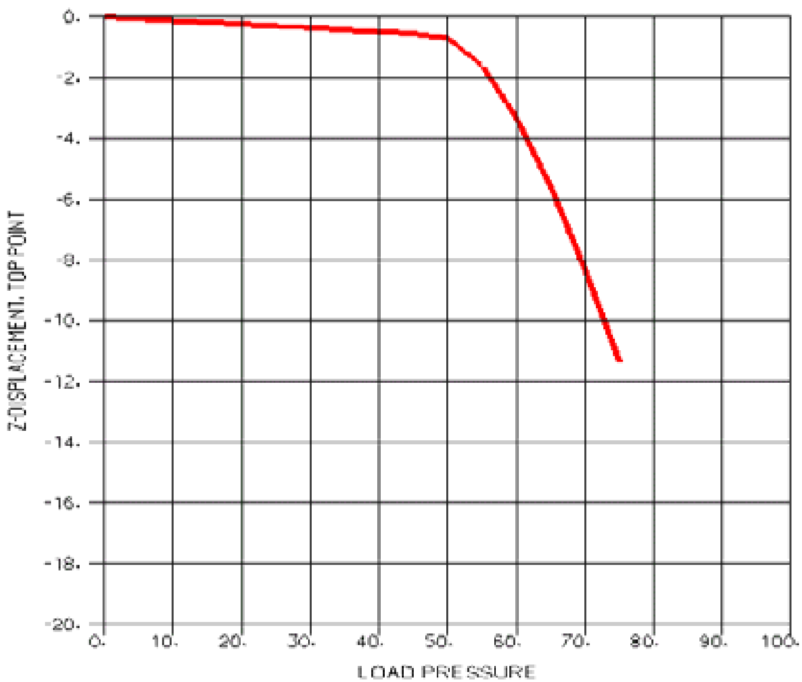

Figure 40. Load-displacement curve results.

6. CONCLUDING REMARKS

The BEM 3D analysis of the canister design models show that with the maximum load of 44 MPa considered in the design premises, the cast iron insert is safe in terms of fracture initiation and growth, due to the dominance of compressive stress field, small magnitude of induced tensile stresses and adequate fracture toughness of the cast iron material.

The 2D FEM plastic analysis shows similar distribution patterns and magnitudes of stresses and plastic strains as reported in SKB literature, but a final collapse load of 75 MPa is reached, lower than that estimated in the SKB literature. The FEM analysis of collapse load considered in this report is the external load at the start of plastic collapse of the insert, not the full load for generating total buckling failure of the ligaments. Such buckling collapse of the insert may occur at a higher external pressure as indicated in SKB literature.

References

Andersson, C.-G., Andersson, M., Erixon, B., Björkegren, L.-E., Dillström, P., Minnebo P., Nillson, K.-F., Nilsson, F. *Probabilistic analysis and material characterisation of canister insert for spent nuclear fuel - Summary report*. SKB TR-05-17, 2005

Broek D. *Elementary engineering fracture mechanics, 4th edition*, Kluwer Academic Publishers, pp.516, 1986.

Dillström, P., *Probablistic analysis of canister inserts for spent nuclear fuel*. SKB TR-05-19, 2005

Nilsson, F. *Personal communication on canister insert's toughness data*, 2005.

Werme, L., *Design premises for canister for spent nuclear fuel*. SKB TR-98-08. Swedish Nuclear Fuel and Waste Management Co. (SKB), Stockholm, 1998.

Zhang, G. *Personal communication on using ADINA, 2006*.

Appendix: Calculated SIF results

Table A1. Calculated stress intensity factor (SIF) at the crack tip (initial crack size of **1 mm**, without deviation of fuel hole position).

Unit: $MN/mm^{3/2}$

Crack 1				Crack 2			
MP	**Mode I**	**Mode II**	**Mode III**	**MP**	**Mode I**	**Mode II**	**Mode III**
1	-78.54932	0.5206448	-0.1965149	16	-45.88329	-1.101484	0.3276130
2	-75.18803	0.4573309	-0.2591365	17	-43.94066	-1.004079	0.4520944
3	-73.26822	0.3808790	-0.3184472	18	-42.84247	-0.880266	0.5710440
4	-72.73228	0.2874462	-0.3732483	19	-42.55671	-0.728845	0.6839500
5	-71.19288	0.1782886	-0.3988901	20	-41.66956	-0.535558	0.7525014
6	-70.43323	0.0655376	-0.4127344	21	-41.23551	-0.328132	0.8031020
7	-70.10371	-0.0466255	-0.4130745	22	-41.05079	-0.114059	0.8300969
8	-70.26540	-0.1565359	-0.4009615	23	-41.15160	0.1045698	0.8345135
9	-70.10035	-0.2521819	-0.3713108	24	-41.05022	0.3143873	0.8027954
10	-70.42629	-0.3376435	-0.3337556	25	-41.23426	0.5119814	0.7512168
11	-71.18115	-0.4124954	-0.2889151	26	-41.66693	0.6955436	0.6798767
12	-72.71596	-0.4751840	-0.2410751	27	-42.55308	0.8600883	0.5957803
13	-73.24662	-0.5068116	-0.1856692	28	-42.83640	0.9723670	0.4794023
14	-75.17190	-0.5309507	-0.1302356	29	-43.93849	1.060449	0.3594397
15	-78.53697	-0.5442922	-0.0744080	30	-45.88405	1.123434	0.2365148
Crack 3				**Crack 4**			
MP	**Mode I**	**Mode II**	**Mode III**	**MP**	**Mode I**	**Mode II**	**Mode III**
31	-45.90794	1.251697	-0.3474196	46	-78.48675	-0.502942	0.1898926
32	-43.96411	1.148589	-0.4898169	47	-75.12829	-0.442203	0.2506959
33	-42.86516	1.015727	-0.6268136	48	-73.21019	-0.366913	0.3078324
34	-42.57902	0.8504982	-0.7571056	49	-72.67488	-0.275785	0.3609621
35	-41.69119	0.6359131	-0.8382926	50	-71.13673	-0.170317	0.3857564
36	-41.25672	0.4047147	-0.8996661	51	-70.37768	-0.060798	0.3990942
37	-41.07174	0.1646496	-0.9348321	52	-70.04840	-0.047840	0.3990980
38	-41.17244	-0.0816563	-0.9447671	53	-70.20991	0.1543687	0.3869451
39	-41.07092	-0.3202258	-0.9137748	54	-70.04485	0.2463912	0.3579470
40	-41.25497	-0.5462168	-0.8600370	55	-70.37041	0.3283825	0.3214092
41	-41.68780	-0.7578141	-0.7834746	56	-71.12448	0.3997476	0.2780867
42	-42.57435	-0.9484974	-0.6920046	57	-72.65796	0.4596698	0.2319992
43	-42.85794	-1.081747	-0.5627632	58	-73.18783	0.4901155	0.1785572
44	-43.96070	-1.188620	-0.4291670	59	-75.11134	0.5124046	0.1249066
45	-45.90734	-1.267592	-0.2913995	60	-78.47350	0.5250119	0.0711019

Table A2. Calculated stress intensity factor (SIF) at the crack tip (initial crack size of **2 mm**, without deviation of fuel hole position).

Unit: $MN/mm^{3/2}$

Crack 1				Crack 2			
MP	**Mode I**	**Mode II**	**Mode III**	**MP**	**Mode I**	**Mode II**	**Mode III**
1	-111.9623	0.7077307	-0.4055870	16	-65.56278	-1.527672	0.5381369
2	-107.4401	0.5756164	-0.4939533	17	-62.97390	-1.369798	0.7094829
3	-105.0992	0.4187969	-0.5771376	18	-61.66773	-1.167960	0.8775548
4	-104.6348	0.2339043	-0.6496514	19	-61.47185	-0.923892	1.033044
5	-102.5775	0.0400415	-0.6647404	20	-60.30069	-0.628892	1.117310
6	-101.5768	-0.1513396	-0.6559885	21	-59.74149	-0.318552	1.171784
7	-101.1819	-0.3327067	-0.6230393	22	-59.53188	-0.003578	1.190457
8	-101.4730	-0.5001567	-0.5688556	23	-59.72010	0.311051	1.175223
9	-101.1753	-0.6242931	-0.4897800	24	-59.53197	0.599771	1.109207
10	-101.5635	-0.7234104	-0.4029116	25	-59.74166	0.865841	1.017129
11	-102.5576	-0.7971819	-0.3111557	26	-60.30091	1.105678	0.9006742
12	-104.6072	-0.8458859	-0.2218671	27	-61.47205	1.315005	0.7695697
13	-105.0683	-0.8392201	-0.1378874	28	-61.66777	1.444006	0.6028610
14	-107.4058	-0.8241474	-0.0566124	29	-62.97374	1.539481	0.4307380
15	-111.9242	-0.7929816	0.0182272	30	-65.56242	1.594853	0.2631245
Crack 3				**Crack 4**			
MP	**Mode I**	**Mode II**	**Mode III**	**MP**	**Mode I**	**Mode II**	**Mode III**
31	-65.59797	1.738564	-0.566058	46	-111.8755	-0.681700	0.3972405
32	-63.00723	1.573860	-0.761873	47	-107.3573	-0.552068	0.4828578
33	-61.69985	1.358702	-0.955422	48	-105.0186	-0.397907	0.5627440
34	-61.50324	1.094725	-1.135230	49	-104.5550	-0.216873	0.6326642
35	-60.33089	0.770164	-1.237437	50	-102.4993	-0.027856	0.6461650
36	-59.77088	0.426927	-1.307144	51	-101.4993	0.1594062	0.6363884
37	-59.56069	0.075610	-1.337456	52	-101.1046	0.3358316	0.6027300
38	-59.74854	-0.277891	-1.330102	53	-101.3953	0.4982210	0.5483389
39	-59.56005	-0.607194	-1.265388	54	-101.0973	0.6167381	0.4699282
40	-59.76959	-0.913483	-1.170511	55	-101.4848	0.7106096	0.3843097
41	-60.32890	-1.193005	-1.046948	56	-102.4775	0.7789709	0.2945629
42	-61.50039	-1.439468	-0.905603	57	-104.5248	0.8238263	0.2074953
43	-61.69648	-1.598436	-0.721018	58	-104.9848	0.8143808	0.1265696
44	-63.00332	-1.720713	-0.529576	59	-107.3199	0.7964769	0.0480409
45	-65.59346	-1.797937	-0.341724	60	-111.8340	0.7643760	-0.023664

Table A3. Calculated stress intensity factor (SIF) at the crack tip (initial crack size of **5 mm**, without deviation of fuel hole position).

Unit: MN/mm$^{3/2}$

Crack 1				Crack 2			
MP	**Mode I**	**Mode II**	**Mode III**	**MP**	**Mode I**	**Mode II**	**Mode III**
1	-181.8771	0.9954417	-1.265816	16	-107.2435	-2.316552	1.210505
2	-175.9909	0.5574629	-1.416173	17	-103.9980	-1.932832	1.485756
3	-173.5461	0.0700882	-1.541287	18	-102.8011	-1.474147	1.744008
4	-174.0857	-0.4842415	-1.632996	19	-103.4060	-0.933963	1.971296
5	-171.2408	-0.9878059	-1.551109	20	-101.8543	-0.354405	2.041088
6	-170.0077	-1.452765	-1.397220	21	-101.2283	0.2271405	2.043305
7	-169.6758	-1.852228	-1.179514	22	-101.1139	0.7862867	1.974311
8	-170.3994	-2.177527	-0.9098416	23	-101.6078	1.314573	1.841516
9	-169.6506	-2.317007	-0.6000775	24	-101.1158	1.732903	1.630120
10	-169.9576	-2.363769	-0.2963793	25	-101.2320	2.084393	1.389015
11	-171.1649	-2.321511	-0.0100970	26	-101.8592	2.367831	1.124451
12	-173.9826	-2.204701	0.2380822	27	-103.4132	2.582897	0.8574598
13	-173.4315	-1.934579	0.3958748	28	-102.8081	2.637358	0.5836921
14	-175.8642	-1.671403	0.5323741	29	-104.0043	2.650065	0.3099665
15	-181.7388	-1.395089	0.6442661	30	-107.2500	2.606586	0.0478928
Crack 3				**Crack 4**			
MP	**Mode I**	**Mode II**	**Mode III**	**MP**	**Mode I**	**Mode II**	**Mode III**
31	-107.3006	2.645664	-1.252468	46	-181.7466	-0.952516	1.253188
32	-104.0515	2.249497	-1.566096	47	-175.8661	-0.520168	1.399453
33	-102.8520	1.769313	-1.862845	48	-173.4246	-0.037091	1.520792
34	-103.4549	1.197300	-2.127337	49	-173.9655	0.5111660	1.608166
35	-101.9002	0.5737531	-2.224785	50	-171.1224	1.009843	1.523772
36	-101.2720	-0.0584815	-2.251032	51	-169.8897	1.468181	1.367364
37	-101.1557	-0.6732025	-2.200548	52	-169.5574	1.860261	1.147709
38	-101.6480	-1.261380	-2.080640	53	-170.2797	2.177468	0.8768021
39	-101.1547	-1.742282	-1.872388	54	-169.5296	2.308148	0.5672346
40	-101.2699	-2.156336	-1.628151	55	-169.8344	2.346065	0.2646584
41	-101.8965	-2.501791	-1.353870	56	-171.0387	2.295027	-0.019419
42	-103.4502	-2.777084	-1.071809	57	-173.8517	2.168904	-0.264215
43	-102.8457	-2.879863	-0.7713015	58	-173.2981	1.894070	-0.417479
44	-104.0432	-2.935570	-0.4673872	59	-175.7263	1.626144	-0.548541
45	-107.2909	-2.928010	-0.1733283	60	-181.5940	1.347036	-0.654812

Table A4. Calculated stress intensity factor (SIF) at the crack tip (initial crack size of **10 mm**, without deviation of fuel hole position).

Unit: $MN/mm^{3/2}$

Crack 1				Crack 2			
MP	**Mode I**	**Mode II**	**Mode III**	**MP**	**Mode I**	**Mode II**	**Mode III**
1	-271.9643	1.096242	-3.365979	16	-161.9051	-3.035293	2.642090
2	-264.8447	-0.1088616	-3.597195	17	-158.2620	-2.129459	3.034755
3	-263.0039	-1.394228	-3.756909	18	-157.8113	-1.119449	3.379480
4	-266.2490	-2.833786	-3.831377	19	-160.4869	0.03722377	3.659362
5	-262.9717	-4.045043	-3.452602	20	-158.8563	1.149449	3.596624
6	-261.9078	-5.111618	-2.884871	21	-158.4793	2.210001	3.385901
7	-261.9945	-5.963211	-2.161431	22	-158.7375	3.165026	3.035150
8	-263.5419	-6.577887	-1.318011	23	-159.8318	3.996275	2.566412
9	-261.9244	-6.633704	-0.4152490	24	-158.7480	4.490347	1.988798
10	-261.7681	-6.424899	0.4335857	25	-158.4993	4.810514	1.397964
11	-262.7608	-5.965742	1.193485	26	-158.8849	4.960827	0.8144041
12	-265.9570	-5.309064	1.812010	27	-160.5232	4.962227	0.2819291
13	-262.6745	-4.272002	2.100403	28	-157.8433	4.642023	-0.134086
14	-264.4763	-3.309158	2.315995	29	-158.2880	4.309604	-0.526615
15	-271.5517	-2.344028	2.462689	30	-161.9236	3.913924	-0.888921
Crack 3				**Crack 4**			
MP	**Mode I**	**Mode II**	**Mode III**	**MP**	**Mode I**	**Mode II**	**Mode III**
31	-161.9891	3.481317	-2.698833	46	-271.7929	-1.045217	3.351436
32	-158.3392	2.558307	-3.142961	47	-264.6814	0.1572321	3.577993
33	-157.8830	1.517733	-3.539188	48	-262.8457	1.438904	3.731999
34	-160.5537	0.3169665	-3.868648	49	-266.0931	2.871839	3.799825
35	-158.9167	-0.8535335	-3.843497	50	-262.8168	4.078099	3.416407
36	-158.5345	-1.981639	-3.665745	51	-261.7521	5.136577	2.843904
37	-158.7881	-3.011119	-3.340805	52	-261.8366	5.978334	2.116354
38	-159.8781	-3.923092	-2.890547	53	-263.3806	6.581484	1.269777
39	-158.7906	-4.502237	-2.319141	54	-261.7592	6.623929	0.3659984
40	-158.5387	-4.908506	-1.726062	55	-261.5976	6.401193	-0.482341
41	-158.9213	-5.145280	-1.131200	56	-262.5837	5.927757	-1.239905
42	-160.5568	-5.232158	-0.5800399	57	-265.7707	5.255539	-1.854173
43	-157.8776	-4.982109	-0.1286867	58	-262.4824	4.210126	-2.135705
44	-158.3238	-4.713416	0.3048914	59	-264.2758	3.239081	-2.343053
45	-161.9617	-4.372522	0.7121691	60	-271.3393	2.268556	-2.480596

Table A5. Calculated stress intensity factor (SIF) at the crack tip (initial crack size of **1 mm**, with fuel hole deviation of **1 mm**).

Unit: MN/mm$^{3/2}$

Crack 1				**Crack 2**			
MP	**Mode I**	**Mode II**	**Mode III**	**MP**	**Mode I**	**Mode II**	**Mode III**
1	-77.58473	0.5148772	-0.1870255	16	-46.19113	-1.185048	0.3308130
2	-74.27032	0.4545769	-0.2490795	17	-44.23499	-1.087097	0.4658123
3	-72.38031	0.3810829	-0.3080074	18	-43.12876	-0.959817	0.5954088
4	-71.85834	0.2907111	-0.3625940	19	-42.84016	-0.802164	0.7188714
5	-70.34093	0.1844323	-0.3888471	20	-41.94660	-0.598379	0.7955046
6	-69.59301	0.0743923	-0.4036291	21	-41.50927	-0.378639	0.8532396
7	-69.26943	-0.0353915	-0.4052362	22	-41.32302	-0.150816	0.8859140
8	-69.43064	-0.1432827	-0.3946714	23	-41.42427	0.0828158	0.8945611
9	-69.26603	-0.2377311	-0.3668914	24	-41.32239	0.3083877	0.8644734
10	-69.58600	-0.3225158	-0.3312578	25	-41.50788	0.5218002	0.8129368
11	-70.32911	-0.3972266	-0.2883438	26	-41.94376	0.7211475	0.7399864
12	-71.84188	-0.4602487	-0.2423346	27	-42.83624	0.9009142	0.6530303
13	-72.35860	-0.4932915	-0.1885401	28	-43.12237	1.025907	0.5307300
14	-74.25395	-0.5191296	-0.1345247	29	-44.23253	1.125742	0.4042409
15	-77.57202	-0.5345740	-0.0799278	30	-46.19158	1.199706	0.2740586
Crack 3				**Crack 4**			
MP	**Mode I**	**Mode II**	**Mode III**	**MP**	**Mode I**	**Mode II**	**Mode III**
31	-46.70115	1.224255	-0.3420478	46	-77.71538	-0.520258	0.1941418
32	-44.72116	1.122549	-0.4814345	47	-74.39179	-0.458280	0.2568984
33	-43.60036	0.9917229	-0.6154876	48	-72.49462	-0.381328	0.3159198
34	-43.30592	0.8291219	-0.7429126	49	-71.96702	-0.288097	0.3708487
35	-42.40133	0.6184483	-0.8219758	50	-70.44497	-0.179834	0.3968402
36	-41.95822	0.3916577	-0.8815235	51	-69.69418	-0.067264	0.4111284
37	-41.76915	0.1563667	-0.9153379	52	-69.36874	0.0445872	0.4117434
38	-41.87087	-0.0848370	-0.9243992	53	-69.52915	0.1544545	0.3998705
39	-41.76827	-0.3180462	-0.8934118	54	-69.36516	0.2497925	0.3706036
40	-41.95636	-0.5387546	-0.8402369	55	-69.68683	0.3349760	0.3334737
41	-42.39777	-0.7452038	-0.7648222	56	-70.43265	0.4093826	0.2892303
42	-43.30101	-0.9310483	-0.6749529	57	-71.94998	0.4720944	0.2419957
43	-43.59283	-1.060464	-0.5484356	58	-72.47214	0.5045994	0.1868370
44	-44.71750	-1.164176	-0.4177313	59	-74.37460	0.5285778	0.1313840
45	-46.70033	-1.240612	-0.2830018	60	-77.70179	0.5424754	0.0756914

Table A6. Calculated stress intensity factor (SIF) at the crack tip (initial crack size of **1 mm**, with fuel hole deviation of **2 mm**).

Unit: MN/mm$^{3/2}$

Crack 1				Crack 2			
MP	**Mode I**	**Mode II**	**Mode III**	**MP**	**Mode I**	**Mode II**	**Mode III**
1	-76.72165	0.5559757	-0.1910661	16	-46.41006	-1.183450	0.3309365
2	-73.44886	0.4949752	-0.2577139	17	-44.44346	-1.085339	0.4658573
3	-71.58515	0.4197448	-0.3212278	18	-43.33081	-0.957948	0.5953240
4	-71.07507	0.3267667	-0.3803637	19	-43.03958	-0.800148	0.7186514
5	-69.57707	0.2156595	-0.4103622	20	-42.14126	-0.596406	0.7950853
6	-68.83951	0.09983982	-0.4286058	21	-41.70142	-0.376762	0.8526023
7	-68.52111	-0.0165000	-0.4330649	22	-41.51393	-0.149109	0.8850397
8	-68.68177	-0.1316765	-0.4247125	23	-41.61537	0.08429393	0.8934603
9	-68.51767	-0.2342457	-0.3978346	24	-41.51319	0.3094753	0.8631915
10	-68.83243	-0.3272714	-0.3622165	25	-41.69982	0.5224590	0.8115295
11	-69.56517	-0.4102494	-0.3183684	26	-42.13812	0.7213441	0.7384930
12	-71.05851	-0.4812808	-0.2706093	27	-43.03534	0.9006549	0.6515121
13	-71.56335	-0.5211432	-0.2131006	28	-43.32403	1.025187	0.5293401
14	-73.43232	-0.5528028	-0.1550825	29	-44.44064	1.124660	0.4029915
15	-76.70873	-0.5732706	-0.0961889	30	-46.41027	1.198316	0.2729579
Crack 3				**Crack 4**			
MP	**Mode I**	**Mode II**	**Mode III**	**MP**	**Mode I**	**Mode II**	**Mode III**
31	-47.48412	1.216843	-0.3745436	46	-76.82506	-0.5498935	0.1811225
32	-45.46776	1.105080	-0.5111233	47	-73.54184	-0.4920428	0.2484449
33	-44.32465	0.9660191	-0.6415854	48	-71.66896	-0.4175158	0.3124053
34	-44.02115	0.7965965	-0.7649185	49	-71.15041	-0.3252024	0.3724467
35	-43.09961	0.5808958	-0.8389937	50	-69.64696	-0.2157588	0.4031231
36	-42.64766	0.3503345	-0.8931103	51	-68.90567	-0.1009078	0.4219787
37	-42.45429	0.1127047	-0.9211954	52	-68.58465	0.01428358	0.4268258
38	-42.55680	-0.1294374	-0.9243111	53	-68.74373	0.1284781	0.4188173
39	-42.45329	-0.3617112	-0.8873627	54	-68.58086	0.2291563	0.3926087
40	-42.64556	-0.5800713	-0.8284309	55	-68.89793	0.3202981	0.3579573
41	-43.09567	-0.7827211	-0.7475488	56	-69.63406	0.4012706	0.3155572
42	-44.01572	-0.9634868	-0.6526455	57	-71.13259	0.4709171	0.2696003
43	-44.31650	-1.085956	-0.5219989	58	-71.64567	0.5103770	0.2144141
44	-45.46350	-1.181302	-0.3876905	59	-73.52368	0.5416653	0.1585294
45	-47.48268	-1.247546	-0.2501644	60	-76.81033	0.5634607	0.1018318

Table A7. Calculated stress intensity factor (SIF) at the crack tip (initial crack size of **1 mm**, with fuel hole deviation of **5 mm**).

Unit: MN/mm$^{3/2}$

Crack 1				Crack 2			
MP	**Mode I**	**Mode II**	**Mode III**	**MP**	**Mode I**	**Mode II**	**Mode III**
1	-73.88091	0.6142962	-0.1951836	16	-47.21243	-1.314193	0.3674518
2	-70.74726	0.5533159	-0.2676836	17	-45.21022	-1.205419	0.5170083
3	-68.97251	0.4769959	-0.3371113	18	-44.07653	-1.064339	0.6605275
4	-68.50471	0.3821916	-0.4022643	19	-43.77817	-0.889689	0.7972332
5	-67.07181	0.2656609	-0.4379509	20	-42.86366	-0.663833	0.8821319
6	-66.36919	0.1429006	-0.4617806	21	-42.41573	-0.420287	0.9461319
7	-66.06854	0.01819483	-0.4712104	22	-42.22467	-0.167755	0.9823876
8	-66.22796	-0.1067537	-0.4670998	23	-42.32766	0.09126392	0.9920294
9	-66.06485	-0.2213261	-0.4426070	24	-42.22445	0.3415159	0.9587103
10	-66.36164	-0.3268931	-0.4079379	25	-42.41517	0.5783223	0.9015692
11	-67.05922	-0.4227701	-0.3634436	26	-42.86205	0.7995468	0.8206301
12	-68.48722	-0.5064925	-0.3135813	27	-43.77597	0.9990465	0.7240985
13	-68.94980	-0.5578060	-0.2503845	28	-44.07204	1.137834	0.5882375
14	-70.72942	-0.5989978	-0.1861261	29	-45.20998	1.248597	0.4477337
15	-73.86634	-0.6274979	-0.1205318	30	-47.21548	1.330489	0.3031585
Crack 3				**Crack 4**			
MP	**Mode I**	**Mode II**	**Mode III**	**MP**	**Mode I**	**Mode II**	**Mode III**
31	-49.82346	1.224305	-0.3490439	46	-74.61916	-0.5319364	0.1786655
32	-47.70102	1.119978	-0.4886693	47	-71.43544	-0.4746824	0.2439178
33	-46.49409	0.9865110	-0.6227840	48	-69.62212	-0.4012598	0.3058269
34	-46.16686	0.8210065	-0.7500632	49	-69.12522	-0.3105005	0.3638490
35	-45.19629	0.6080514	-0.8280886	50	-67.66778	-0.2035011	0.3930323
36	-44.71920	0.3793546	-0.8862215	51	-66.95003	-0.0914393	0.4105914
37	-44.51405	0.1426510	-0.9183421	52	-66.64001	0.02071259	0.4144561
38	-44.61983	-0.0994281	-0.9254996	53	-66.79595	0.1316442	0.4057776
39	-44.51311	-0.3323310	-0.8925624	54	-66.63637	0.2289074	0.3794693
40	-44.71720	-0.5521775	-0.8375919	55	-66.94259	0.3166784	0.3450675
41	-45.19248	-0.7572486	-0.7606048	56	-67.65535	0.3943608	0.3032781
42	-46.16160	-0.9412992	-0.6694989	57	-69.10804	0.4608998	0.2582096
43	-46.48603	-1.068176	-0.5425384	58	-69.59966	0.4978458	0.2045852
44	-47.69707	-1.169541	-0.4115777	59	-71.41799	0.5269722	0.1503601
45	-49.82254	-1.243595	-0.2767526	60	-74.60509	0.5468926	0.09542035

Table A8. Calculated stress intensity factor (SIF) at the crack tip (initial crack size of **1 mm**, with fuel hole deviation of **10 mm**).

Unit: MN/mm$^{3/2}$

Crack 1				**Crack 2**			
MP	**Mode I**	**Mode II**	**Mode III**	**MP**	**Mode I**	**Mode II**	**Mode III**
1	-68.55639	0.6162875	-0.1598099	16	-48.77733	-1.576593	0.4528176
2	-65.68492	0.5681685	-0.2317934	17	-46.70480	-1.442956	0.6307758
3	-64.07843	0.5045750	-0.3016064	18	-45.52923	-1.271621	0.8012990
4	-63.69152	0.4233473	-0.3680963	19	-45.21597	-1.060997	0.9635731
5	-62.38120	0.3173661	-0.4091477	20	-44.26892	-0.788991	1.064051
6	-61.74452	0.2033512	-0.4400352	21	-43.80438	-0.496029	1.139574
7	-61.47743	0.0849973	-0.4577788	22	-43.60557	-0.192461	1.181886
8	-61.63476	-0.0361557	-0.4629161	23	-43.71079	0.1187179	1.192302
9	-61.47300	-0.1523890	-0.4478661	24	-43.60505	0.4196833	1.151053
10	-61.73549	-0.2622587	-0.4219195	25	-43.80324	0.7042960	1.081077
11	-62.36652	-0.3649455	-0.3851079	26	-44.26643	0.9699685	0.9823542
12	-63.67113	-0.4574411	-0.3413943	27	-45.21254	1.209187	0.8647391
13	-64.05273	-0.5211297	-0.2806967	28	-45.52330	1.375106	0.6993803
14	-65.66331	-0.5740774	-0.2180187	29	-46.70309	1.506300	0.5285632
15	-68.53725	-0.6146852	-0.1531224	30	-48.77875	1.601730	0.3531113
Crack 3				**Crack 4**			
MP	**Mode I**	**Mode II**	**Mode III**	**MP**	**Mode I**	**Mode II**	**Mode III**
31	-53.33746	1.237597	-0.3938241	46	-70.77034	-0.612919	0.1978455
32	-51.05388	1.119086	-0.5332028	47	-67.76126	-0.550128	0.2722171
33	-49.74913	0.9727476	-0.6660361	48	-66.05305	-0.469257	0.3429522
34	-49.38393	0.7950208	-0.7912402	49	-65.59533	-0.369058	0.4094247
35	-48.33857	0.5714142	-0.8646869	50	-64.21847	-0.249231	0.4443111
36	-47.82277	0.3333719	-0.9171296	51	-63.54201	-0.123123	0.4664644
37	-47.59915	0.08904701	-0.9425741	52	-63.25125	0.00386799	0.4733678
38	-47.70916	-0.1588819	-0.9422308	53	-63.40170	0.1302828	0.4662024
39	-47.59790	-0.3945657	-0.9010524	54	-63.24717	0.2430783	0.4388222
40	-47.82014	-0.6150780	-0.8378028	55	-63.53370	0.3458443	0.4018138
41	-48.33375	-0.8186637	-0.7526432	56	-64.20480	0.4378589	0.3558425
42	-49.37729	-0.9992386	-0.6538500	57	-65.57643	0.5175890	0.3054789
43	-49.73937	-1.119107	-0.5201677	58	-66.02884	0.5643997	0.2437753
44	-51.04841	-1.211764	-0.3830984	59	-67.74150	0.6016278	0.1810785
45	-53.33511	-1.274770	-0.2430453	60	-70.75342	0.6278603	0.1172974

Table A9. Calculated stress intensity factor (SIF) at the crack tip (initial crack size of **2 mm**, with fuel hole devisaion of **1 mm**).

Unit: MN/mm$^{3/2}$

Crack 1				Crack 2			
MP	**Mode I**	**Mode II**	**Mode III**	**MP**	**Mode I**	**Mode II**	**Mode III**
1	-110.6335	0.7005122	-0.3870466	16	-65.99759	-1.644632	0.5443017
2	-106.1807	0.5742503	-0.4744778	17	-63.38944	-1.485817	0.7301070
3	-103.8856	0.4232419	-0.5572159	18	-62.07221	-1.278703	0.9132716
4	-103.4470	0.2444525	-0.6294914	19	-61.87210	-1.025266	1.083545
5	-101.4225	0.05610911	-0.6460794	20	-60.69184	-0.715147	1.178971
6	-100.4399	-0.1301288	-0.6395336	21	-60.12784	-0.387210	1.243171
7	-100.0549	-0.3071525	-0.6094781	22	-59.91597	-0.052646	1.269522
8	-100.3466	-0.4710576	-0.5587238	23	-60.10472	0.2832193	1.259885
9	-100.0481	-0.5935669	-0.4836560	24	-59.91585	0.5940110	1.195820
10	-100.4265	-0.6921500	-0.4008128	25	-60.12758	0.8822067	1.103494
11	-101.4022	-0.7665900	-0.3129363	26	-60.69139	1.143966	0.9845358
12	-103.4189	-0.8169048	-0.2272037	27	-61.87140	1.374412	0.8492006
13	-103.8541	-0.8140905	-0.1460672	28	-62.07124	1.520901	0.6741384
14	-106.1458	-0.8032519	-0.0672821	29	-63.38818	1.632526	0.4926844
15	-110.5946	-0.7770324	0.00578266	30	-65.99601	1.702317	0.3152209
Crack 3				**Crack 4**			
MP	**Mode I**	**Mode II**	**Mode III**	**MP**	**Mode I**	**Mode II**	**Mode III**
31	-66.71084	1.699804	-0.5604099	46	-110.7916	-0.705544	0.4036015
32	-64.06888	1.536205	-0.7521555	47	-106.3224	-0.574084	0.4918634
33	-62.73142	1.323140	-0.9415082	48	-104.0122	-0.417412	0.5743776
34	-62.52219	1.062066	-1.117223	49	-103.5599	-0.233233	0.6467462
35	-61.32603	0.7423792	-1.216101	50	-101.5269	-0.040207	0.6618356
36	-60.75341	0.4048243	-1.282805	51	-100.5388	0.1513813	0.6532723
37	-60.53718	0.0598795	-1.310691	52	-100.1496	0.3323339	0.6203488
38	-60.72624	-0.2866352	-1.301529	53	-100.4388	0.4993830	0.5662217
39	-60.53643	-0.6082351	-1.236233	54	-100.1422	0.6224581	0.4873359
40	-60.75188	-0.9067439	-1.141614	55	-100.5241	0.7207022	0.4008036
41	-61.32369	-1.178538	-1.019199	56	-101.5048	0.7931959	0.3097071
42	-62.51886	-1.417571	-0.8797599	57	-103.5294	0.8418405	0.2209833
43	-62.72750	-1.570295	-0.6988985	58	-103.9780	0.8351626	0.1376661
44	-64.06437	-1.687360	-0.5115373	59	-106.2845	0.8195010	0.05657776
45	-66.70565	-1.760440	-0.3278814	60	-110.7495	0.7890098	-0.0177129

Table A10. Calculated stress intensity factor (SIF) at the crack tip (initial crack size of **2 mm**, with fuel hole deviation of **2 mm**).

Unit: $MN/mm^{3/2}$

Crack 1				Crack 2			
MP	**Mode I**	**Mode II**	**Mode III**	**MP**	**Mode I**	**Mode II**	**Mode III**
1	-109.4414	0.7595348	-0.3869002	16	-66.30282	-1.641865	0.5459008
2	-105.0501	0.6346792	-0.4806032	17	-63.67994	-1.482262	0.7315794
3	-102.7935	0.4836162	-0.5699613	18	-62.35386	-1.274356	0.9145379
4	-102.3766	0.3034613	-0.6490712	19	-62.14969	-1.020038	1.084547
5	-100.3811	0.1100253	-0.6720435	20	-60.96269	-0.709438	1.179429
6	-99.41490	-0.0829957	-0.6717229	21	-60.39508	-0.381190	1.242958
7	-99.03853	-0.2683906	-0.6472590	22	-60.18144	-0.046543	1.268552
8	-99.33064	-0.4421621	-0.6013202	23	-60.37042	0.2891708	1.258120
9	-99.03160	-0.5766424	-0.5291978	24	-60.18133	0.5992678	1.193336
10	-99.40114	-0.6878597	-0.4479001	25	-60.39485	0.8865692	1.100420
11	-100.3604	-0.7753734	-0.3600215	26	-60.96230	1.147250	0.9810259
12	-102.3480	-0.8387554	-0.2728401	27	-62.14907	1.376521	0.8454483
13	-102.7613	-0.8478671	-0.1868194	28	-62.35299	1.521639	0.6705989
14	-105.0144	-0.8475199	-0.1023644	29	-63.67880	1.632088	0.4894401
15	-109.4017	-0.8302140	-0.0233783	30	-66.30140	1.700844	0.3123047
Crack 3				**Crack 4**			
MP	**Mode I**	**Mode II**	**Mode III**	**MP**	**Mode I**	**Mode II**	**Mode III**
31	-67.80429	1.688891	-0.6085361	46	-109.5420	-0.747222	0.3850537
32	-65.11009	1.510538	-0.7964681	47	-105.1298	-0.621705	0.4795874
33	-63.74097	1.284844	-0.9807828	48	-102.8528	-0.468646	0.5690821
34	-63.51688	1.013220	-1.150659	49	-102.4139	-0.285847	0.6486428
35	-62.29620	0.6856978	-1.242134	50	-100.4070	-0.091277	0.6703496
36	-61.71026	0.3422242	-1.300695	51	-99.43250	0.1034113	0.6682439
37	-61.48738	-0.0064795	-1.319900	52	-99.04960	0.2889764	0.6413491
38	-61.67700	-0.3545999	-1.301698	53	-99.33694	0.4620337	0.5927425
39	-61.48629	-0.6748130	-1.227301	54	-99.04161	0.5925869	0.5182667
40	-61.70808	-0.9697391	-1.123888	55	-99.41660	0.6992330	0.4353402
41	-62.29287	-1.235729	-0.9931679	56	-100.3831	0.7809877	0.3469545
42	-63.51220	-1.466964	-0.8461203	57	-102.3808	0.8394637	0.2601331
43	-63.73557	-1.608929	-0.6591980	58	-102.8158	0.8427445	0.1768580
44	-65.10395	-1.713096	-0.4666451	59	-105.0889	0.8375928	0.09516271
45	-67.79732	-1.771123	-0.2790797	60	-109.4966	0.8180318	0.01957709

Table A11. Calculated stress intensity factor (SIF) at the crack tip (initial crack size of **2 mm**, with fuel hole deviation of **5 mm**).

Unit: $MN/mm^{3/2}$

Crack 1				Crack 2			
MP	**Mode I**	**Mode II**	**Mode III**	**MP**	**Mode I**	**Mode II**	**Mode III**
1	-105.5357	0.8456531	-0.3737682	16	-67.43355	-1.824696	0.6020753
2	-101.3518	0.7282310	-0.4751981	17	-64.76138	-1.649305	0.8078786
3	-99.23087	0.5831325	-0.5732724	18	-63.40772	-1.420597	1.010760
4	-98.89354	0.4084094	-0.6616974	19	-63.19426	-1.140845	1.199373
5	-96.99570	0.2132982	-0.6960710	20	-61.98509	-0.797890	1.305506
6	-96.08492	0.01530254	-0.7080108	21	-61.40634	-0.435057	1.377228
7	-95.73828	-0.1786415	-0.6957322	22	-61.18805	-0.064640	1.407149
8	-96.03291	-0.3645440	-0.6614526	23	-61.37958	0.3074891	1.397275
9	-95.73055	-0.5178080	-0.5983284	24	-61.18912	0.6525682	1.327032
10	-96.06954	-0.6502016	-0.5234550	25	-61.40846	0.9728419	1.225315
11	-96.97253	-0.7608192	-0.4389726	26	-61.98823	1.264009	1.093878
12	-98.86153	-0.8481726	-0.3520416	27	-63.19852	1.520553	0.9440462
13	-99.19502	-0.8814213	-0.2587086	28	-63.41229	1.684306	0.7496437
14	-101.3120	-0.9018577	-0.1655351	29	-64.76626	1.809083	0.5481381
15	-105.4915	-0.9025335	-0.0769838	30	-67.43880	1.887248	0.3510374
Crack 3				**Crack 4**			
MP	**Mode I**	**Mode II**	**Mode III**	**MP**	**Mode I**	**Mode II**	**Mode III**
31	-71.08991	1.697678	-0.5796887	46	-106.4384	-0.721362	0.3823506
32	-68.24612	1.526952	-0.7718894	47	-102.1659	-0.596246	0.4739871
33	-66.78999	1.306524	-0.9611556	48	-99.96926	-0.444387	0.5604827
34	-66.53079	1.037499	-1.136214	49	-99.56150	-0.263445	0.6371074
35	-65.24094	0.7117372	-1.232000	50	-97.61935	-0.072132	0.6565680
36	-64.61869	0.3691935	-1.294590	51	-96.67867	0.1187840	0.6524567
37	-64.37882	0.02066555	-1.317596	52	-96.31153	0.3001607	0.6239580
38	-64.57272	-0.3279037	-1.303014	53	-96.59468	0.4686672	0.5741687
39	-64.37799	-0.6482311	-1.232240	54	-96.30387	0.5942877	0.4993310
40	-64.61701	-0.9439153	-1.132608	55	-96.66343	0.6960008	0.4165626
41	-65.23836	-1.211447	-1.005866	56	-97.59636	0.7729075	0.3288773
42	-66.52714	-1.445082	-0.8630624	57	-99.52975	0.8267653	0.2432053
43	-66.78572	-1.590385	-0.6811435	58	-99.93374	0.8261538	0.1621175
44	-68.24122	-1.700521	-0.4932522	59	-102.1265	0.8176570	0.08277343
45	-71.08429	-1.766784	-0.3095996	60	-106.3948	0.7952769	0.00957320

Table A12. Calculated stress intensity factor (SIF) at the crack tip (initial crack size of **2 mm**, with fuel hole deviation of **10 mm**).

Unit: $MN/mm^{3/2}$

Crack 1				**Crack 2**			
MP	**Mode I**	**Mode II**	**Mode III**	**MP**	**Mode I**	**Mode II**	**Mode III**
1	-98.22695	0.8575589	-0.2825814	16	-69.63969	-2.190911	0.7295881
2	-94.43507	0.7731896	-0.3826949	17	-66.86917	-1.979807	0.9743744
3	-92.57199	0.6618178	-0.4820514	18	-65.45932	-1.706104	1.215647
4	-92.38815	0.5228840	-0.5743201	19	-65.22491	-1.372873	1.439956
5	-90.67494	0.3550569	-0.6233385	20	-63.96996	-0.962955	1.567060
6	-89.86922	0.1793980	-0.6544031	21	-63.36729	-0.528983	1.653545
7	-89.57922	0.00135402	-0.6646051	22	-63.13784	-0.085377	1.690353
8	-89.87926	-0.1755716	-0.6551703	23	-63.33233	0.3608904	1.679719
9	-89.56923	-0.3346246	-0.6171918	24	-63.13808	0.7769408	1.596450
10	-89.84934	-0.4798678	-0.5654182	25	-63.36775	1.163730	1.474906
11	-90.64499	-0.6099598	-0.5009986	26	-63.97060	1.515982	1.317013
12	-92.34680	-0.7220061	-0.4298805	27	-65.22571	1.826688	1.136230
13	-92.52568	-0.7892643	-0.3421924	28	-65.46003	2.026291	0.8999089
14	-94.38372	-0.8420524	-0.2521330	29	-66.86975	2.177157	0.6549501
15	-98.16993	-0.8748643	-0.1640337	30	-69.64017	2.270429	0.4153769
Crack 3				**Crack 4**			
MP	**Mode I**	**Mode II**	**Mode III**	**MP**	**Mode I**	**Mode II**	**Mode III**
31	-76.01298	1.713096	-0.6550097	46	-101.0355	-0.834007	0.4098925
32	-72.93997	1.518352	-0.8469824	47	-97.00924	-0.701360	0.5138879
33	-71.34789	1.275011	-1.034265	48	-94.95610	-0.538848	0.6127589
34	-71.02951	0.9838467	-1.205808	49	-94.60655	-0.344430	0.7010216
35	-69.63281	0.6394404	-1.293082	50	-92.77793	-0.135158	0.7283521
36	-68.95350	0.2808092	-1.344967	51	-91.89676	0.0753516	0.7305214
37	-68.68600	-0.0805319	-1.355398	52	-91.55728	0.2774702	0.7061730
38	-68.88439	-0.4384466	-1.326775	53	-91.83307	0.4675623	0.6584094
39	-68.68440	-0.7617424	-1.240900	54	-91.54825	0.6148375	0.5820605
40	-68.95031	-1.056452	-1.126384	55	-91.87879	0.7375247	0.4956379
41	-69.62796	-1.319073	-0.9853784	56	-92.75083	0.8344435	0.4021341
42	-71.02274	-1.544271	-0.8295711	57	-94.56911	0.9067891	0.3090449
43	-71.34015	-1.674818	-0.6374789	58	-94.91420	0.9201149	0.2167085
44	-72.93125	-1.767851	-0.4406200	59	-96.96284	0.9229610	0.1253567
45	-76.00314	-1.814163	-0.2498200	60	-100.9840	0.9089329	0.04008107

Table A13. Calculated stress intensity factor (SIF) at the crack tip (initial crack size of **5 mm**, with fuel hole deviation of **1 mm**).

Unit: $MN/mm^{3/2}$

Crack 1				Crack 2			
MP	**Mode I**	**Mode II**	**Mode III**	**MP**	**Mode I**	**Mode II**	**Mode III**
1	-179.9244	0.9882710	-1.213061	16	-107.9268	-2.499048	1.226496
2	-174.1610	0.5668921	-1.361728	17	-104.6518	-2.111168	1.524896
3	-171.8039	0.09666140	-1.485790	18	-103.4377	-1.641551	1.806678
4	-172.4098	-0.4395837	-1.577352	19	-104.0352	-1.083750	2.056663
5	-169.6247	-0.9276136	-1.500867	20	-102.4685	-0.478653	2.142770
6	-168.4280	-1.378624	-1.354693	21	-101.8344	0.1318853	2.158758
7	-168.1178	-1.766614	-1.146626	22	-101.7159	0.7225657	2.100123
8	-168.8481	-2.083174	-0.8881426	23	-102.2102	1.284500	1.974347
9	-168.0920	-2.220514	-0.5909999	24	-101.7169	1.736706	1.764407
10	-168.3767	-2.268626	-0.2995613	25	-101.8362	2.121695	1.521546
11	-169.5471	-2.231182	-0.0247837	26	-102.4706	2.438037	1.251974
12	-172.3043	-2.122195	0.2134121	27	-104.0385	2.684556	0.9776238
13	-171.6867	-1.866716	0.3642728	28	-103.4406	2.764502	0.6907985
14	-174.0316	-1.618774	0.4954688	29	-104.6537	2.800625	0.4025965
15	-179.7833	-1.358489	0.6034811	30	-107.9285	2.778005	0.1252468
Crack 3				**Crack 4**			
MP	**Mode I**	**Mode II**	**Mode III**	**MP**	**Mode I**	**Mode II**	**Mode III**
31	-109.0265	2.583404	-1.252956	46	-180.0574	-0.988016	1.264938
32	-105.6979	2.185695	-1.560332	47	-174.2515	-0.551873	1.415158
33	-104.4496	1.705345	-1.850458	48	-171.8544	-0.063991	1.540256
34	-105.0279	1.134237	-2.108247	49	-172.4156	0.4900646	1.630987
35	-103.4338	0.5154863	-2.198913	50	-169.6091	0.9953379	1.548567
36	-102.7840	-0.1101753	-2.218423	51	-168.3960	1.460617	1.393474
37	-102.6567	-0.7165593	-2.161757	52	-168.0730	1.859758	1.174360
38	-103.1497	-1.294673	-2.036379	53	-168.7935	2.184076	0.9032571
39	-102.6553	-1.762793	-1.824515	54	-168.0449	2.321394	0.5924985
40	-102.7810	-2.163188	-1.578218	55	-168.3400	2.365576	0.2881333
41	-103.4287	-2.494299	-1.303611	56	-169.5244	2.320391	0.0016797
42	-105.0213	-2.755139	-1.022881	57	-172.3003	2.199612	-0.245870
43	-104.4413	-2.844273	-0.7276581	58	-171.7262	1.928500	-0.402727
44	-105.6873	-2.888233	-0.4299310	59	-174.1098	1.663505	-0.537712
45	-109.0142	-2.870719	-0.1426249	60	-179.9025	1.386369	-0.648010

Table A14. Calculated stress intensity factor (SIF) at the crack tip (initial crack size of **5 mm**, with fuel hole deviation of **2 mm**).

Unit: $MN/mm^{3/2}$

Crack 1				Crack 2			
MP	**Mode I**	**Mode II**	**Mode III**	**MP**	**Mode I**	**Mode II**	**Mode III**
1	- 178.1749	1.086741	-1.189276	16	-108.3938	-2.492336	1.237081
2	-172.5184	0.6765782	-1.347115	17	-105.0958	-2.100105	1.535360
3	-170.2424	0.2155281	-1.482078	18	-103.8669	-1.625908	1.816793
4	-170.9113	-0.3130775	-1.585621	19	-104.4559	-1.062901	2.066173
5	-168.1819	-0.8018023	-1.523589	20	-102.8780	-0.454078	2.150074
6	-167.0197	-1.257607	-1.392858	21	-102.2376	0.1594405	2.163069
7	-166.7303	-1.654820	-1.200126	22	-102.1159	0.7520479	2.100868
8	-167.4676	-1.985037	-0.9564098	23	-102.6101	1.314753	1.971129
9	-166.7041	-2.143675	-0.6709873	24	-102.1169	1.764925	1.757348
10	-166.9675	-2.216093	-0.3883604	25	-102.2395	2.146760	1.511137
11	-168.1028	-2.205568	-0.1189968	26	-102.8803	2.458937	1.238882
12	-170.8036	-2.124822	0.1173248	27	-104.4596	2.700649	0.9627082
13	-170.1228	-1.898075	0.2749724	28	-103.8700	2.774525	0.6760846
14	-172.3863	-1.675878	0.4148654	29	-105.0980	2.805386	0.3883277
15	-178.0305	-1.438645	0.5332708	30	-108.3959	2.777905	0.1115881
Crack 3				**Crack 4**			
MP	**Mode I**	**Mode II**	**Mode III**	**MP**	**Mode I**	**Mode II**	**Mode III**
31	-110.6981	2.564231	-1.338825	46	-178.1173	-1.054056	1.233989
32	-107.2851	2.140468	-1.639749	47	-172.3986	-0.627470	1.394407
33	-105.9814	1.637531	-1.921308	48	-170.0539	-0.145501	1.530552
34	-106.5265	1.047394	-2.169027	49	-170.6400	0.4061669	1.632533
35	-104.8901	0.4144466	-2.246555	50	-167.8754	0.9134267	1.560513
36	-104.2161	-0.2220324	-2.251559	51	-166.6844	1.383089	1.415657
37	-104.0757	-0.8353950	-2.179431	52	-166.3717	1.788954	1.206179
38	-104.5670	-1.416703	-2.037892	53	-167.0896	2.122215	0.9440269
39	-104.0729	-1.882827	-1.809636	54	-166.3412	2.270900	0.6406512
40	-104.2105	-2.277302	-1.547422	55	-166.6235	2.328011	0.3424751
41	-104.8810	-2.598449	-1.257632	56	-167.7833	2.297297	0.0608823
42	-106.5144	-2.845670	-0.9628803	57	-170.5145	2.192066	-0.183043
43	-105.9670	-2.915384	-0.6564862	58	-169.9143	1.937241	-0.339178
44	-107.2679	-2.936035	-0.3492917	59	-172.2442	1.689481	-0.474517
45	-110.6787	-2.891502	-0.0548353	60	-177.9485	1.430389	-0.586298

Table A15. Calculated stress intensity factor (SIF) at the crack tip (initial crack size of **5 mm**, with fuel hole deviation of **5 mm**).

Unit: $MN/mm^{3/2}$

Crack 1				**Crack 2**			
MP	**Mode I**	**Mode II**	**Mode III**	**MP**	**Mode I**	**Mode II**	**Mode III**
1	-172.4884	1.243164	-1.077848	16	-110.1742	-2.776763	1.343592
2	-167.2018	0.8774157	-1.247620	17	-106.8049	-2.353095	1.673803
3	-165.2023	0.4594683	-1.398631	18	-105.5372	-1.839545	1.985889
4	-166.0862	-0.0252475	-1.522096	19	-106.1144	-1.229422	2.263152
5	-163.5400	-0.4908804	-1.494121	20	-104.5034	-0.564709	2.361526
6	-162.4905	-0.9340756	-1.402999	21	-103.8472	0.1071067	2.383400
7	-162.2693	-1.331019	-1.252677	22	-103.7197	0.7584436	2.323446
8	-163.0298	-1.673679	-1.052637	23	-104.2196	1.379616	2.189684
9	-162.2399	-1.869533	-0.8065059	24	-103.7253	1.883381	1.962547
10	-162.4320	-1.989775	-0.5568647	25	-103.8582	2.314275	1.698179
11	-163.4514	-2.036699	-0.3126238	26	-104.5196	2.670511	1.403202
12	-165.9654	-2.019778	-0.0921520	27	-106.1372	2.950284	1.101612
13	-165.0681	-1.866261	0.07236021	28	-105.5619	3.047269	0.7834087
14	-167.0534	-1.710006	0.2241015	29	-106.8309	3.094373	0.4632837
15	-172.3258	-1.533337	0.3583926	30	-110.2027	3.075577	0.1548946
Crack 3				**Crack 4**			
MP	**Mode I**	**Mode II**	**Mode III**	**MP**	**Mode I**	**Mode II**	**Mode III**
31	-115.8113	2.569576	-1.327249	46	-173.2619	-1.010058	1.234064
32	-112.1694	2.144635	-1.635700	47	-167.7542	-0.582326	1.389775
33	-110.7282	1.636112	-1.924765	48	-165.5334	-0.100300	1.521115
34	-111.2083	1.034836	-2.179273	49	-166.1734	0.4507583	1.618390
35	-109.4592	0.3935297	-2.257429	50	-163.5135	0.9544984	1.542100
36	-108.7248	-0.2505074	-2.260614	51	-162.3782	1.419635	1.392986
37	-108.5550	-0.8697206	-2.184838	52	-162.0923	1.819937	1.179607
38	-109.0509	-1.454759	-2.038352	53	-162.8053	2.14661	0.9140051
39	-108.5533	-1.917065	-1.805334	54	-162.0630	2.286815	0.6084976
40	-108.7213	-2.305729	-1.539776	55	-162.3198	2.335026	0.3092060
41	-109.4533	-2.619551	-1.248585	56	-163.4251	2.295135	0.02762983
42	-111.2005	-2.858905	-0.9549950	57	-166.0530	2.180926	-0.2152147
43	-110.7185	-2.918790	-0.6559863	58	-165.3996	1.917492	-0.3678761
44	-112.1573	-2.935350	-0.3565709	59	-167.6065	1.662415	-0.4994930
45	-115.7977	-2.891199	-0.0696432	60	-173.1003	1.396990	-0.6074776

Table A16. Calculated stress intensity factor (SIF) at the crack tip (initial crack size of **5 mm**, with fuel hole deviation of **10 mm**).

Unit: MN/mm$^{3/2}$

Crack 1				Crack 2			
MP	**Mode I**	**Mode II**	**Mode III**	**MP**	**Mode I**	**Mode II**	**Mode III**
1	-161.9121	1.304307	-0.7478221	16	-113.6454	-3.344390	1.575289
2	-157.3306	1.057692	-0.9140343	17	-110.1289	-2.853001	1.967451
3	-155.8659	0.7617665	-1.071348	18	-108.7768	-2.256892	2.338998
4	-157.1742	0.4058652	-1.210921	19	-109.3202	-1.549416	2.670423
5	-154.9779	0.03650418	-1.238143	20	-107.6353	-0.770063	2.796543
6	-154.1454	-0.3286028	-1.218080	21	-106.9399	0.0212049	2.834727
7	-154.0563	-0.6711950	-1.150324	22	-106.7934	0.7926922	2.777518
8	-154.8638	-0.9844318	-1.041074	23	-107.2967	1.533291	2.633677
9	-154.0180	-1.204112	-0.8862673	24	-106.7958	2.146148	2.377358
10	-154.0692	-1.373312	-0.7202208	25	-106.9444	2.676634	2.073969
11	-154.8627	-1.493160	-0.5485924	26	-107.6417	3.122006	1.730584
12	-157.0166	-1.567711	-0.3852552	27	-109.3295	3.478554	1.375018
13	-155.6903	-1.539751	-0.2402363	28	-108.7865	3.620622	0.9895089
14	-157.1366	-1.503055	-0.0982167	29	-110.1384	3.697623	0.6001951
15	-161.6988	-1.443920	0.0363388	30	-113.6557	3.691878	0.2240422
Crack 3				**Crack 4**			
MP	**Mode I**	**Mode II**	**Mode III**	**MP**	**Mode I**	**Mode II**	**Mode III**
31	-123.4128	2.578936	-1.501699	46	-164.8672	-1.182702	1.277653
32	-119.4107	2.096682	-1.809510	47	-159.7368	-0.742386	1.452170
33	-117.7437	1.532222	-2.093591	48	-157.7432	-0.243259	1.601742
34	-118.1025	0.8754238	-2.339085	49	-158.4913	0.3289872	1.715762
35	-116.1743	0.1898173	-2.394374	50	-156.0151	0.8597272	1.651000
36	-115.3406	-0.4916035	-2.368803	51	-154.9779	1.354250	1.511163
37	-115.1192	-1.139184	-2.259644	52	-154.7389	1.785549	1.303994
38	-115.6148	-1.743196	-2.076222	53	-155.4431	2.144610	1.041561
39	-115.1145	-2.206285	-1.804596	54	-154.7044	2.317789	0.7342485
40	-115.3310	-2.585590	-1.501993	55	-154.9091	2.398235	0.4298910
41	-116.1593	-2.880081	-1.176345	56	-155.9111	2.389525	0.1398687
42	-118.0824	-3.091707	-0.8526167	57	-158.3491	2.304597	-0.114020
43	-117.7203	-3.108063	-0.5337820	58	-157.5847	2.064120	-0.283731
44	-119.3837	-3.077895	-0.2179726	59	-159.5615	1.827547	-0.433922
45	-123.3829	-2.982743	0.08103455	60	-164.6748	1.575847	-0.560938

Table A17. Calculated stress intensity factor (SIF) at the crack tip (initial crack size of **10 mm**, with fuel hole deviation of **1 mm**).

Unit: $MN/mm^{3/2}$

Crack 1				**Crack 2**			
MP	**Mode I**	**Mode II**	**Mode III**	**MP**	**Mode I**	**Mode II**	**Mode III**
1	-269.5142	1.095810	-3.238495	16	-162.8749	-3.286342	2.681262
2	-262.6059	-0.0690487	-3.467526	17	-159.1867	-2.367707	3.106145
3	-260.9410	-1.313814	-3.626608	18	-158.7082	-1.335642	3.482876
4	-264.3395	-2.709829	-3.702095	19	-161.3705	-0.147678	3.793148
5	-261.1656	-3.885341	-3.338216	20	-159.7171	1.004309	3.749967
6	-260.1695	-4.920473	-2.790775	21	-159.3271	2.108393	3.554641
7	-260.3006	-5.747018	-2.091982	22	-159.5782	3.109235	3.214137
8	-261.8703	-6.343556	-1.276594	23	-160.6717	3.987938	2.750793
9	-260.2288	-6.397560	-0.4047247	24	-159.5857	4.527128	2.171262
10	-260.0265	-6.195331	-0.4145105	25	-159.3414	4.890946	1.574645
11	-260.9498	-5.751063	1.147082	26	-159.7370	5.083288	0.9814874
12	-264.0408	-5.116326	1.742320	27	-161.3951	5.124276	0.4370885
13	-260.6043	-4.117701	2.015814	28	-158.7274	4.834421	0.0028449
14	-262.2298	-3.193184	2.220028	29	-159.1991	4.530453	-0.409624
15	-269.0934	-2.268286	2.358648	30	-162.8787	4.160517	-0.793150
Crack 3				**Crack 4**			
MP	**Mode I**	**Mode II**	**Mode III**	**MP**	**Mode I**	**Mode II**	**Mode III**
31	-164.3864	3.391066	-2.720683	46	-269.4255	-1.090215	3.371369
32	-160.6123	2.458629	-3.156407	47	-262.4282	0.1195461	3.602971
33	-160.0737	1.410308	-3.543174	48	-260.6650	1.409736	3.761443
34	-162.6966	0.2026423	-3.862360	49	-263.9492	2.852455	3.832919
35	-160.9992	-0.9673728	-3.824163	50	-260.7274	4.068549	3.451121
36	-160.5827	-2.091275	-3.632441	51	-259.6924	5.136984	2.879176
37	-160.8175	-3.112522	-3.293603	52	-259.7920	5.988487	2.151054
38	-161.9054	-4.012229	-2.829952	53	-261.3350	6.601090	1.302876
39	-160.8188	-4.572025	-2.247675	54	-259.7135	6.651682	0.3964668
40	-160.5845	-4.956085	-1.646387	55	-259.5358	6.436418	-0.455152
41	-161.0002	-5.168138	-1.046442	56	-260.4912	5.969771	-1.216599
42	-162.6946	-5.228870	-0.4934831	57	-263.6225	5.303673	-1.835044
43	-160.0625	-4.951650	-0.0481967	58	-260.2970	4.262037	-2.121269
44	-160.5904	-4.658706	0.3773560	59	-262.0175	3.293912	-2.333866
45	-164.3517	-4.295890	0.7750079	60	-268.9664	2.325036	-2.476931

Table A18. Calculated stress intensity factor (SIF) at the crack tip (initial crack size of **10 mm**, with fuel hole deviation of **2 mm**).

Unit: MN/mm$^{3/2}$

Crack 1				Crack 2			
MP	**Mode I**	**Mode II**	**Mode III**	**MP**	**Mode I**	**Mode II**	**Mode III**
1	-267.3370	1.247570	-3.145473	16	-163.5222	-3.272006	2.716318
2	-260.6269	0.1192576	-3.388551	17	-159.7969	-2.338846	3.141786
3	-259.1309	-1.091936	-3.565428	18	-159.2927	-1.291149	3.518659
4	-262.6830	-2.455441	-3.662223	19	-161.9393	-0.084870	3.828227
5	-259.6085	-3.616320	-3.329412	20	-160.2692	1.080724	3.778527
6	-258.6783	-4.646174	-2.816856	21	-159.8700	2.196058	3.573904
7	-258.8536	-5.478001	-2.154448	22	-160.1162	3.204782	3.222030
8	-260.4465	-6.090496	-1.375746	23	-161.2094	4.087674	2.745799
9	-258.7807	-6.179407	-0.5359103	24	-160.1241	4.621737	2.153433
10	-258.5330	-6.020501	0.2567152	25	-159.8849	4.976608	1.545390
11	-259.3891	-5.627195	0.9693085	26	-160.2900	5.156475	0.9428508
12	-262.3792	-5.048474	1.552030	27	-161.9649	5.182540	0.3918434
13	-258.7882	-4.111577	1.831813	28	-159.3129	4.872813	-0.041992
14	-260.2438	-3.243825	2.046448	29	-159.8102	4.551961	-0.453218
15	-266.9080	-2.372594	2.199178	30	-163.5273	4.166579	-0.835204
Crack 3				**Crack 4**			
MP	**Mode I**	**Mode II**	**Mode III**	**MP**	**Mode I**	**Mode II**	**Mode III**
31	-166.6641	3.362771	-2.852871	46	-266.7174	-1.183334	3.325416
32	-162.7524	2.390759	-3.279167	47	-259.8542	0.1257008	3.571244
33	-162.1154	1.309107	-3.652413	48	-258.1774	1.294223	3.745024
34	-164.6720	0.07440252	-3.955416	49	-261.5080	2.733106	3.832009
35	-162.9090	-1.116238	-3.897103	50	-258.3479	3.950955	3.464543
36	-162.4537	-2.255700	-3.683574	51	-257.3461	5.024342	2.906919
37	-162.6656	-3.286928	-3.321776	52	-257.4617	5.883999	2.192501
38	-163.7470	-4.191194	-2.834341	53	-259.0022	6.507828	1.357302
39	-162.6632	-4.749371	-2.227827	54	-257.3768	6.573209	0.4621361
40	-162.4480	-5.126218	-1.602694	55	-257.1767	6.375216	-0.379690
41	-162.8986	-5.325230	-0.9795572	56	-258.0922	5.928361	-1.133031
42	-164.6542	-5.367436	-0.4045097	57	-261.1540	5.283982	-1.744975
43	-162.0865	-5.062932	0.0601408	58	-257.7782	4.266332	-2.028663
44	-162.7110	-4.735211	0.5020770	59	-259.4084	3.323983	-2.240405
45	-166.6084	-4.330295	0.9115300	60	-266.2188	2.382855	-2.384549

Table A19. Calculated stress intensity factor (SIF) at the crack tip (initial crack size of **10 mm**, with fuel hole deviation of **5 mm**).

Unit: $MN/mm^{3/2}$

Crack 1				Crack 2			
MP	**Mode I**	**Mode II**	**Mode III**	**MP**	**Mode I**	**Mode II**	**Mode III**
1	-260.3324	1.507071	-2.806031	16	-166.0625	-3.663598	2.906051
2	-254.2811	0.5089197	-3.062773	17	-162.2350	-2.670618	3.376063
3	-253.3427	-0.5743061	-3.267373	18	-161.6745	-1.553376	3.793622
4	-257.3981	-1.807118	-3.405034	19	-164.3050	-0.267303	4.138816
5	-254.6434	-2.885551	-3.153276	20	-162.5898	0.9867037	4.102205
6	-253.9258	-3.858784	-2.737231	21	-162.1699	2.191579	3.901372
7	-254.2425	-4.664613	-2.180503	22	-162.4097	3.287745	3.542895
8	-255.9098	-5.282546	-1.512818	23	-163.5132	4.254834	3.050542
9	-254.1607	-5.437308	-0.7773802	24	-162.4300	4.861011	2.429291
10	-253.7627	-5.372277	-0.0763177	25	-162.2096	5.278944	1.786495
11	-254.3973	-5.098951	0.5613154	26	-162.6483	5.51229	1.143966
12	-257.0575	-4.659386	1.089842	27	-164.3831	5.581482	0.5507857
13	-252.9588	-3.892617	1.367307	28	-161.7540	5.291053	0.0699984
14	-253.8524	-3.183792	1.593462	29	-162.3145	4.980606	-0.388001
15	-259.8528	-2.465276	1.771545	30	-166.1410	4.595174	-0.814767
Crack 3				**Crack 4**			
MP	**Mode I**	**Mode II**	**Mode III**	**MP**	**Mode I**	**Mode II**	**Mode III**
31	-173.7995	3.348468	-2.924063	46	-259.8828	-1.113584	3.336848
32	-169.5352	2.341391	-3.361738	47	-253.3397	0.0889927	3.576275
33	-168.6702	1.217138	-3.744384	48	-251.8621	1.376463	3.743628
34	-171.1027	-0.0713996	-4.053147	49	-255.2889	2.821652	3.824049
35	-169.1688	-1.301319	-3.980074	50	-252.2856	4.039313	3.448547
36	-168.6185	-2.473517	-3.743492	51	-251.3694	5.110369	2.881816
37	-168.7805	-3.528019	-3.352584	52	-251.5293	5.965118	2.158035
38	-169.8612	-4.445132	-2.831757	53	-253.0681	6.581411	1.313548
39	-168.7808	-4.988839	-2.192362	54	-251.4476	6.633059	0.4109606
40	-168.6182	-5.341027	-1.538966	55	-251.2064	6.419518	-0.436370
41	-169.1667	-5.506272	-0.8940125	56	-252.0395	5.955576	-1.192894
42	-171.0965	-5.508740	-0.3059000	57	-254.9484	5.293650	-1.805471
43	-168.6544	-5.152266	0.1501957	58	-251.4785	4.256580	-2.083877
44	-169.5084	-4.784801	0.5806198	59	-252.9118	3.297980	-2.289880
45	-173.7595	-4.348432	0.9773292	60	-259.4049	2.342477	-2.428341

Table A20. Calculated stress intensity factor (SIF) at the crack tip (initial crack size of **10 mm**, with fuel hole deviation of **10 mm**).

Unit: MN/mm$^{3/2}$

Crack 1				Crack 2			
MP	**Mode I**	**Mode II**	**Mode III**	**MP**	**Mode I**	**Mode II**	**Mode III**
1	-247.4798	1.679880	-1.947722	16	-171.0251	-4.441721	3.304069
2	-242.7002	0.9914435	-2.198354	17	-166.9755	-3.323172	3.861209
3	-242.8544	0.2198516	-2.424424	18	-206.1254	-2.061254	4.359506
4	-247.9149	-0.6877199	-2.611061	19	-168.8556	-0.608887	4.776273
5	-245.7771	-1.526515	-2.505767	20	-167.0291	0.8271211	4.765884
6	-245.4725	-2.308234	-2.274402	21	-166.5486	2.216660	4.571612
7	-246.0658	-2.982940	-1.929462	22	-166.7570	3.493160	4.197971
8	-247.8821	-3.532599	-1.492683	23	-167.8613	4.633879	3.670598
9	-245.9593	-3.747060	-0.9887883	24	-166.7681	5.386704	2.988026
10	-245.2602	-3.804511	-0.5005498	25	-166.5700	5.932582	2.271991
11	-245.4567	-3.713814	-0.0492258	26	-167.0600	6.274089	1.545674
12	-247.4717	-3.504815	0.3307243	27	-168.8955	6.430561	0.8646020
13	-242.3558	-3.056196	0.5533950	28	-166.3184	6.175364	0.2858027
14	-242.1444	-2.653409	0.7518691	29	-167.0078	5.882327	-0.270989
15	-246.8595	-2.240734	0.9297035	30	-171.0514	5.491870	-0.794093
Crack 3				**Crack 4**			
MP	**Mode I**	**Mode II**	**Mode III**	**MP**	**Mode I**	**Mode II**	**Mode III**
31	-184.2919	3.331649	-3.284253	46	-248.1701	-1.344768	3.397191
32	-179.4572	2.202887	-3.720514	47	-242.2082	-0.123554	3.660599
33	-178.2039	0.9605549	-4.091269	48	-241.1053	1.187486	3.850053
34	-180.3982	-0.4461885	-4.378667	49	-244.7320	2.659981	3.949963
35	-178.1884	-1.767477	-4.253556	50	-242.0015	3.911312	3.588725
36	-177.4792	-3.015066	-3.952230	51	-241.2337	5.018934	3.033972
37	-177.5518	-4.124615	-3.487013	52	-241.4682	5.912443	2.318764
38	-178.6170	-5.075714	-2.884835	53	-243.0014	6.569569	1.479430
39	-177.5437	-5.612923	-2.162081	54	-241.3727	6.664732	0.5765764
40	-177.4622	-5.936904	-1.429806	55	-241.0432	6.494849	-0.275336
41	-178.1610	-6.052819	-0.7127628	56	-241.7138	6.074394	-1.041139
42	-180.3569	-5.988587	-0.0629357	57	-244.3335	5.454687	-1.666930
43	-178.1489	-5.532401	0.4301928	58	-240.6556	4.453986	-1.968010
44	-179.3869	-5.060995	0.8894922	59	-241.7058	3.525008	-2.199595
45	-184.2043	-4.512347	1.305046	60	-247.6084	2.592063	-2.364904

Table A21. Calculated stress intensity factor (SIF) at the crack tip (initial crack size of **1 mm**) for unevenly distributed confining pressure (loading) case a).

Unit: MN/mm$^{3/2}$

Crack 1				Crack 2			
MP	**Mode I**	**Mode II**	**Mode III**	**MP**	**Mode I**	**Mode II**	**Mode III**
M87216	-565.8842	-0.0688022	-0.8502170	M87272	-510.0799	0.7291833	1.970861
M87171	-538.0093	-0.3799017	-0.8772306	M87227	-486.5114	1.468451	1.971071
M87217	-521.4904	-0.7067529	-0.8756713	M87273	-472.1632	2.224555	1.900622
M87212	-514.0630	-1.057402	-0.8499187	M87268	-465.9558	3.023774	1.769939
M87198	-501.0181	-1.328288	-0.7059138	M87254	-454.0498	3.594273	1.387507
M87213	-494.4731	-1.549713	-0.5196254	M87269	-448.0866	4.045057	0.8980159
M87214	-491.2011	-1.705870	-0.3031845	M87270	-445.0605	4.328372	0.3441611
M87199	-491.7519	-1.794336	-0.0625164	M87255	-445.5102	4.440379	-0.258887
M87188	-491.1769	-1.738002	0.1807702	M87244	-444.9808	4.193335	-0.852175
M87189	-494.4248	-1.612733	0.4030119	M87245	-448.1411	3.781450	-1.386118
M87190	-500.9975	-1.421162	0.5985768	M87246	-454.2028	3.213985	-1.829165
M87178	-513.9958	-1.177993	0.7542573	M87234	-465.6929	2.523613	-2.168557
M87179	-521.3788	-0.8467304	0.7962823	M87235	-472.3536	1.645017	-2.228994
M87180	-536.9498	-0.5347041	0.8147770	M87236	-486.4030	0.8216564	-2.219000
M87181	-563.6142	-0.2362394	0.8041242	M87237	-510.0446	0.0243720	-2.148225

***MP: Mesh points**

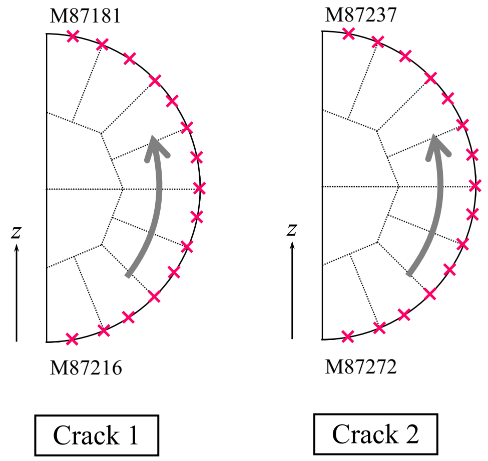

Figure A1. Location and labling of mesh points (nodes) along the fracture tips for laoding case a).

Table A22. Calculated stress intensity factor (SIF) at the crack tip (initial crack size of **1 mm**) for unevenly distributed confining pressure (loading) case b).

Unit: MN/mm$^{3/2}$

Crack 1				**Crack 2**			
***MP**	**Mode I**	**Mode II**	**Mode III**	***MP**	**Mode I**	**Mode II**	**Mode III**
M62406	-528.9605	-17.66232	2.441699	M62462	-529.0929	17.62882	-2.484532
M62361	-504.4506	-17.09486	4.329211	M62417	-504.8802	17.06996	-4.381084
M62407	-489.8394	-16.14843	6.217821	M62463	-489.9881	16.13750	-6.224809
M63560	-482.8420	-14.83652	8.040955	M62458	-482.9022	14.81618	-8.045382
M62388	-470.8867	-12.61422	9.559469	M62444	-471.0053	12.59674	-9.560179
M62403	-464.5686	-10.08181	10.90476	M62459	-464.6384	10.06542	-10.90045
M62404	-461.2701	-7.199433	12.00190	M62460	-461.2956	7.185517	-11.99376
M62389	-461.8039	-4.051764	12.82527	M62445	-461.8191	4.041003	-12.81453
M62378	-461.3539	-0.584684	13.09876	M62434	-461.3635	0.5763648	-13.08613
M62379	-464.5151	2.905719	12.99893	M62435	-464.5204	-2.911810	-12.98460
M62380	-470.7325	6.424594	12.48500	M62436	-470.7337	-6.428617	-12.46863
M62368	-483.1275	9.774579	11.65330	M62424	-483.1100	-9.774837	-11.63401
M62369	-489.6627	12.63433	9.977486	M62425	-489.5397	-12.62156	-9.955879
M62370	-504.5795	15.08738	8.098508	M62426	-504.6751	-15.0439	-8.105994
M62371	-529.6997	16.95302	6.236702	M62427	-529.1468	-16.95286	-6.188643

***MP: Mesh points**

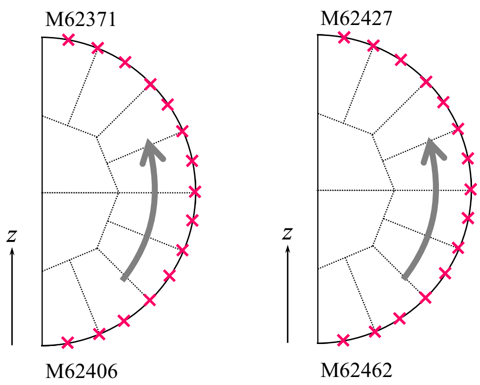

Crack 1 Crack 2

Figure A2 Location and labling of the mesh points (nodes) along the frcature tips for loading acse b).

www.ski.se

STATENS KÄRNKRAFTINSPEKTION
Swedish Nuclear Power Inspectorate

POST/POSTAL ADDRESS SE-106 58 Stockholm
BESÖK/OFFICE Klarabergsviadukten 90
TELEFON/TELEPHONE +46 (0)8 698 84 00
TELEFAX +46 (0)8 661 90 86
E-POST/E-MAIL ski@ski.se
WEBBPLATS/WEB SITE www.ski.se